

Klimaänderung II

0. Rückblick auf das vergangene Wintersemester

Robert Sausen

Institut für Physik der Atmosphäre
Deutsches Zentrum für Luft- und Raumfahrt
Oberpfaffenhofen

Vorlesung SS 2022

LMU München



Knowledge for Tomorrow

Technical information

- <http://www.pa.op.dlr.de/~RobertSausen/vorlesung/index.html>
 - Most recent update on the lecture
 - Slides of the lecture (with some delay)

 - See also LSF <https://lsf.verwaltung.uni-muenchen.de/>

- Contact: robert.sausen@dlr.de

- Further information:
 - www.ipcc.ch
 - www.de-ipcc.de



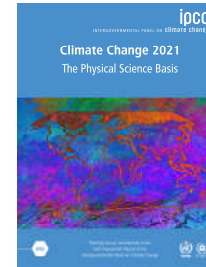
Questions

- Has there been a climate change ?
- What is the impact of man ?
- How will the climate develop in the future ?
- What is necessary to limit climate change?

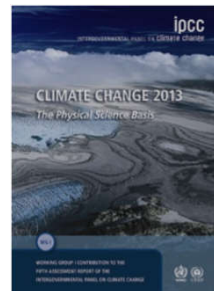


An important source of knowledge: IPCC Assessment Reports

Central results of the recent IPCC Assessment Report
(Sixth Assessment Report "AR6", 2021)



Central results of the recent Fifth IPCC Assessment Report ("AR5", 2013/2014)



Results from the IPCC Special Report (SR15) "Global Warming of 1.5 °C"

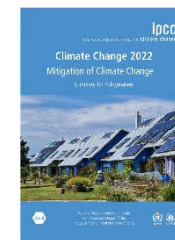
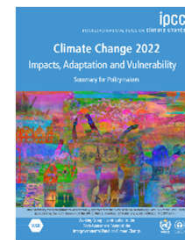
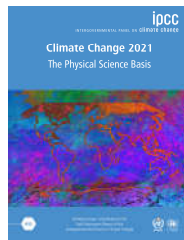


www.ipcc.ch
www.de-ipcc.de



An important source of knowledge: IPCC Assessment Reports

Central results of the recent IPCC Assessment Report (Sixth Assessment Report "AR6", 2021)



Central results of the recent Fifth IPCC Assessment Report ("AR5", 2013/2014)



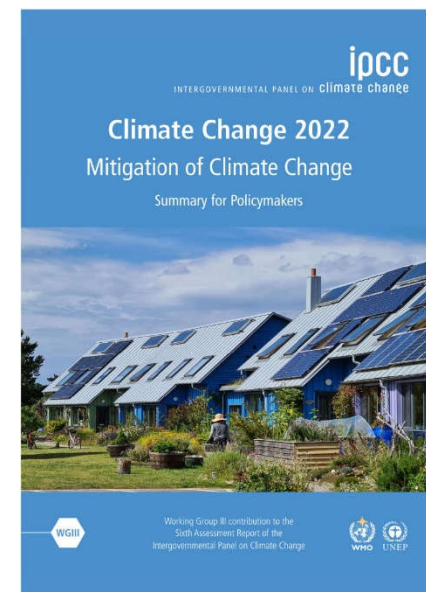
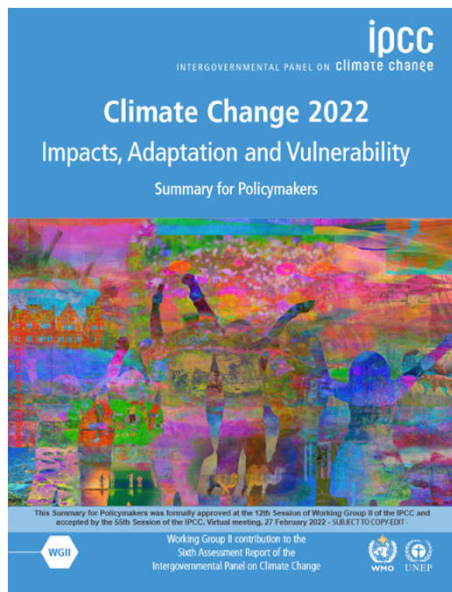
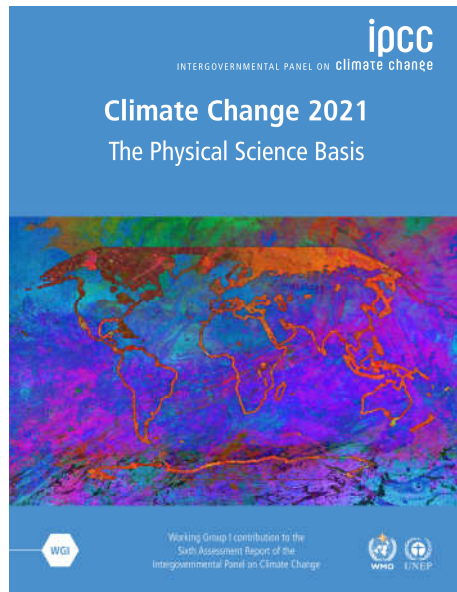
Results from the IPCC Special Report (SR15) "Global Warming of 1.5 °C"



www.ipcc.ch
www.de-ipcc.de

An important source of knowledge: IPCC Assessment Reports

Central results of the recent IPCC Assessment Report (Sixth Assessment Report "AR6", 2021)



What is IPCC (Intergovernmental Panel on Climate Change) 1

The IPCC provides regular assessments of the scientific basis of climate change, its impacts and future risks, and options for adaptation and mitigation.

Created in 1988 by the World Meteorological Organization (WMO) and the United Nations Environment Programme (UNEP), the objective of the IPCC is to provide governments at all levels with scientific information that they can use to develop climate policies. IPCC reports are also a key input into international climate change negotiations. The IPCC is an organization of governments that are members of the United Nations or WMO. The IPCC currently has 195 members. Thousands of people from all over the world contribute to the work of the IPCC. For the assessment reports, IPCC scientists volunteer their time to assess the thousands of scientific papers published each year to provide a comprehensive summary of what is known about the drivers of climate change, its impacts and future risks, and how adaptation and mitigation can reduce those risks. An open and transparent review by experts and governments around the world is an essential part of the IPCC process, to ensure an objective and complete assessment and to reflect a diverse range of views and expertise. Through its assessments, the IPCC identifies the strength of scientific agreement in different areas and indicates where further research is needed. The IPCC does not conduct its own research.



What is IPCC (Intergovernmental Panel on Climate Change) 2

"IPCC assessments provide a scientific basis for governments at all levels to develop climate related policies, and they underlie negotiations at the UN Climate Conference – the United Nations Framework Convention on Climate Change (UNFCCC). **The assessments are policy-relevant but not policy-prescriptive:** they may present projections of future climate change based on different scenarios and the risks that climate change poses and discuss the implications of response options, **but they do not tell policymakers what actions to take.**"

IPCC, 2013



Contents of IPCC AR 6 2021

Working Group I: the Physical Science Basis

Chapters	
Chapter 1: Framing, context, methods	DOWNLOAD
Chapter 2: Changing state of the climate system	DOWNLOAD
Chapter 3: Human influence on the climate system	DOWNLOAD
Chapter 4: Future global climate: scenario-based projections and near-term information	DOWNLOAD
Chapter 5: Global carbon and other biogeochemical cycles and feedbacks	DOWNLOAD
Chapter 6: Short-lived climate forcers	DOWNLOAD
Chapter 7: The Earth's energy budget, climate feedbacks, and climate sensitivity	DOWNLOAD
Chapter 8: Water cycle changes	DOWNLOAD
Chapter 9: Ocean, cryosphere, and sea level change	DOWNLOAD
Chapter 10: Linking global to regional climate change	DOWNLOAD
Chapter 11: Weather and climate extreme events in a changing climate	DOWNLOAD
Chapter 12: Climate change information for regional impact and for risk assessment	DOWNLOAD
Atlas	DOWNLOAD
Supplementary Material	▼
Annexes	▼

<https://www.ipcc.ch/report/ar6/wg1/#FullReport>



Klimaänderung I

1. Rahmen, Kontext, Methoden

Robert Sausen

Institut für Physik der Atmosphäre
Deutsches Zentrum für Luft- und Raumfahrt
Oberpfaffenhofen

Vorlesung WS 2021/22

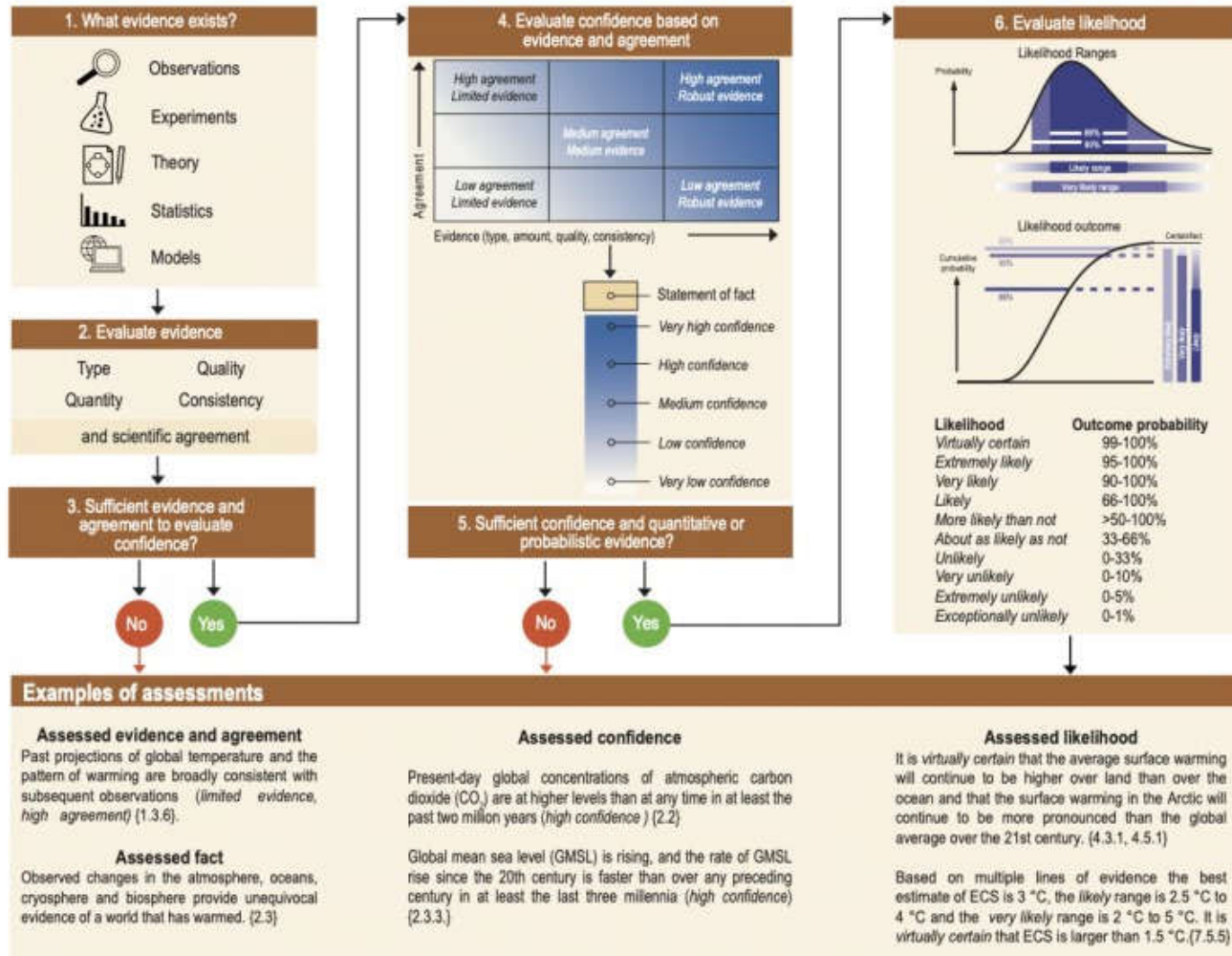
LMU München



Knowledge for Tomorrow

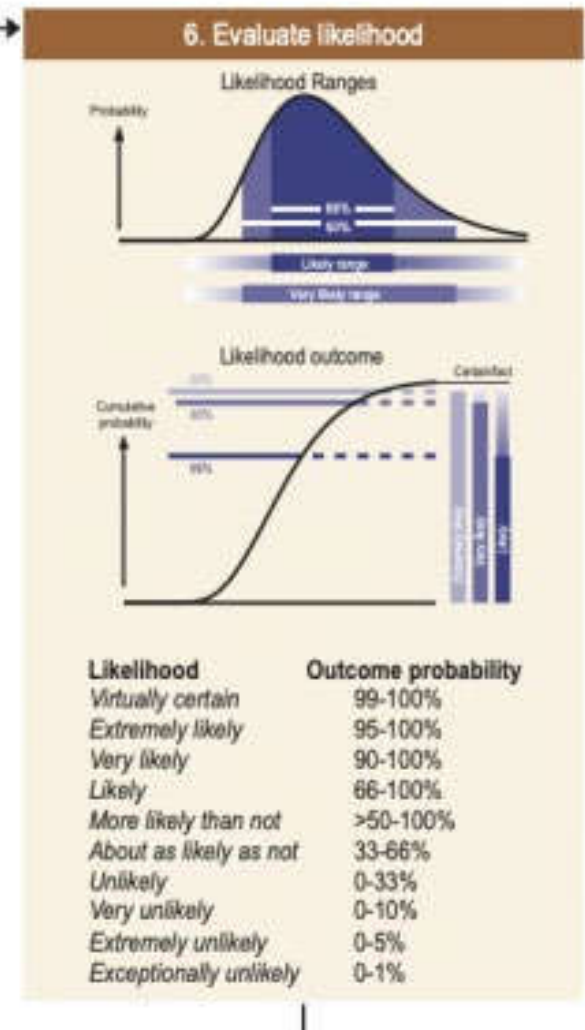
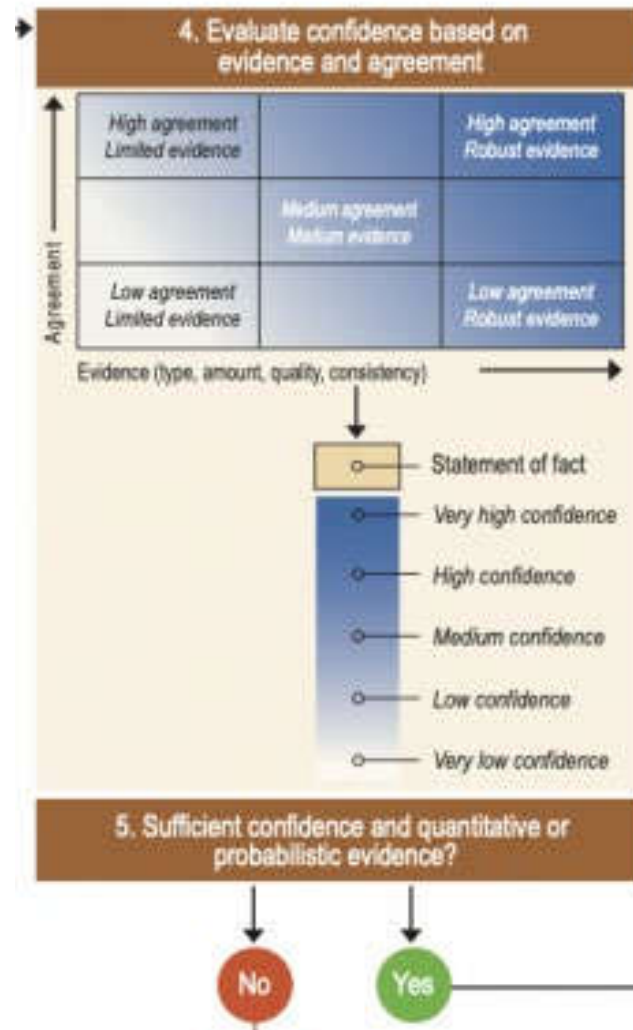
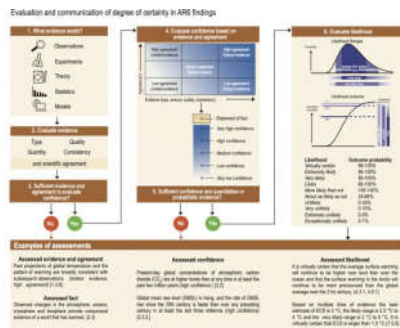


Evaluation and communication of degree of certainty in AR6 findings





IPCC 2021, Chap. 1



Climate science milestones between 1817-2021

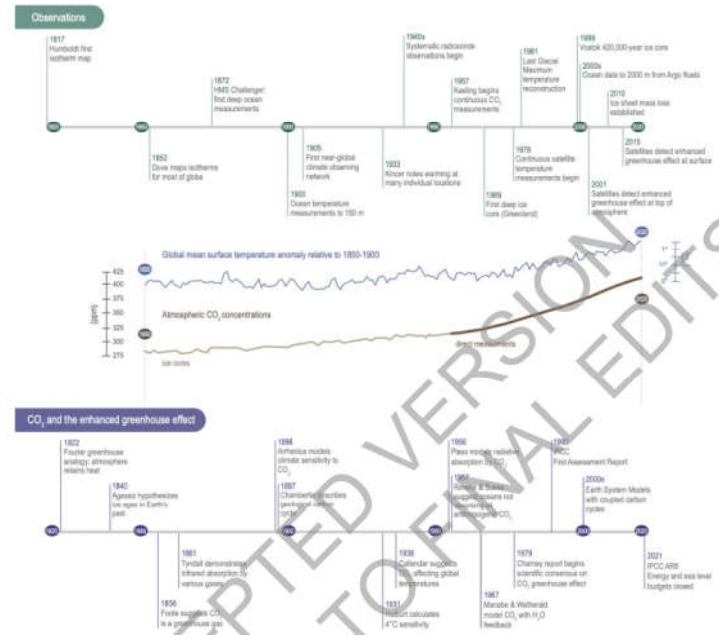
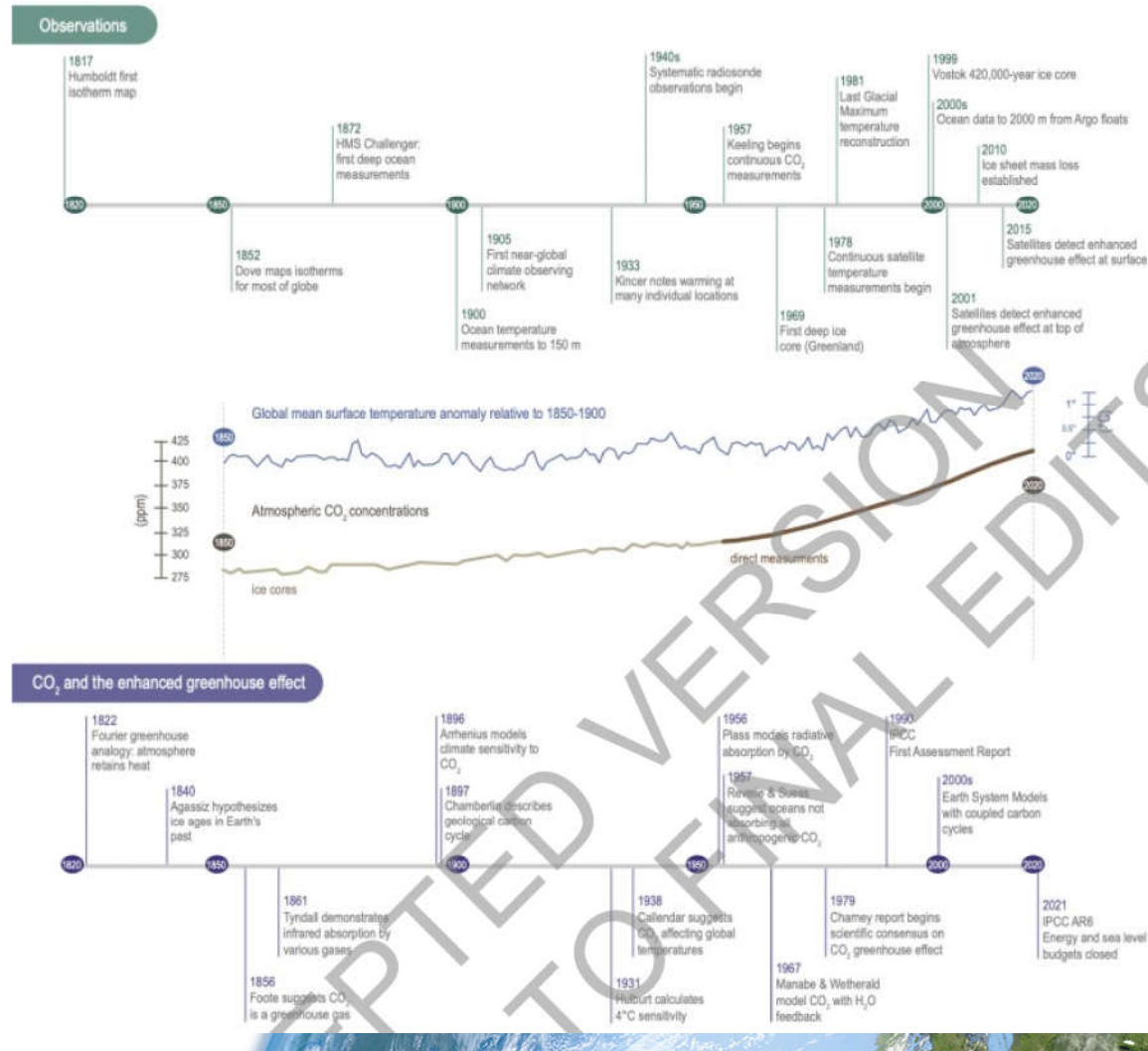
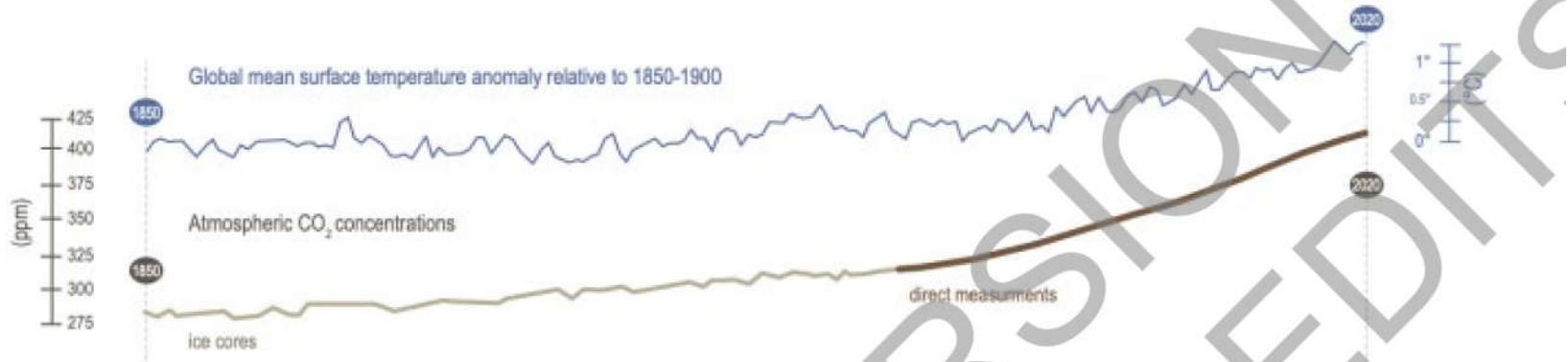
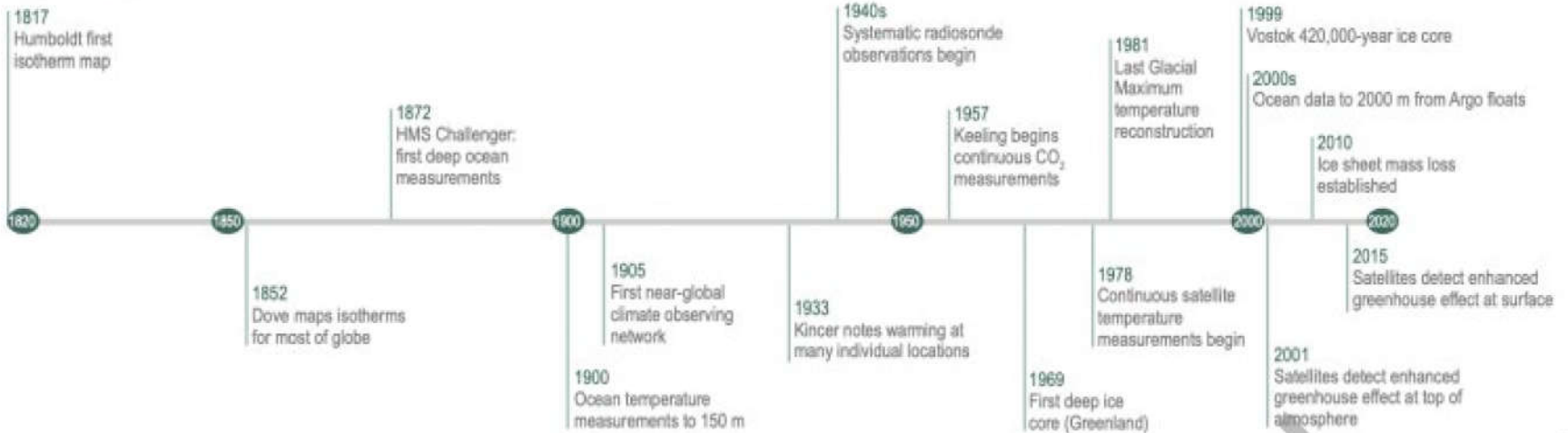
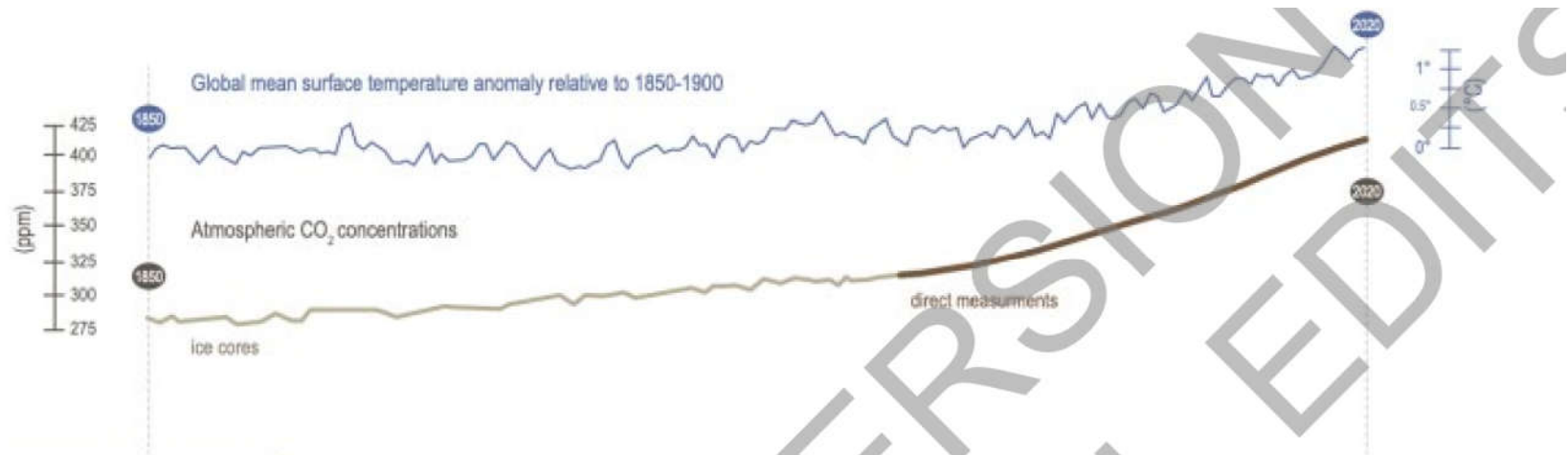


Figure 1.6: Climate science milestones, between 1817-2021. Milestones in observations (top); Curves of global surface air temperature (GMST) using HadCRUT5 (Morice et al., 2021) and atmospheric CO₂ concentrations from Antarctic ice cores (Lüthi et al., 2008; Bereiter et al., 2015) and direct air measurements from 1957 onwards (Tans and Keeling, 2020) (see Figure 1.4 for details) (middle). Milestone in scientific understanding of the CO₂ enhanced greenhouse effect (bottom). Further details on each milestone are available in Chapter 1, Section 1.3, and Chapter 1 of AR4.

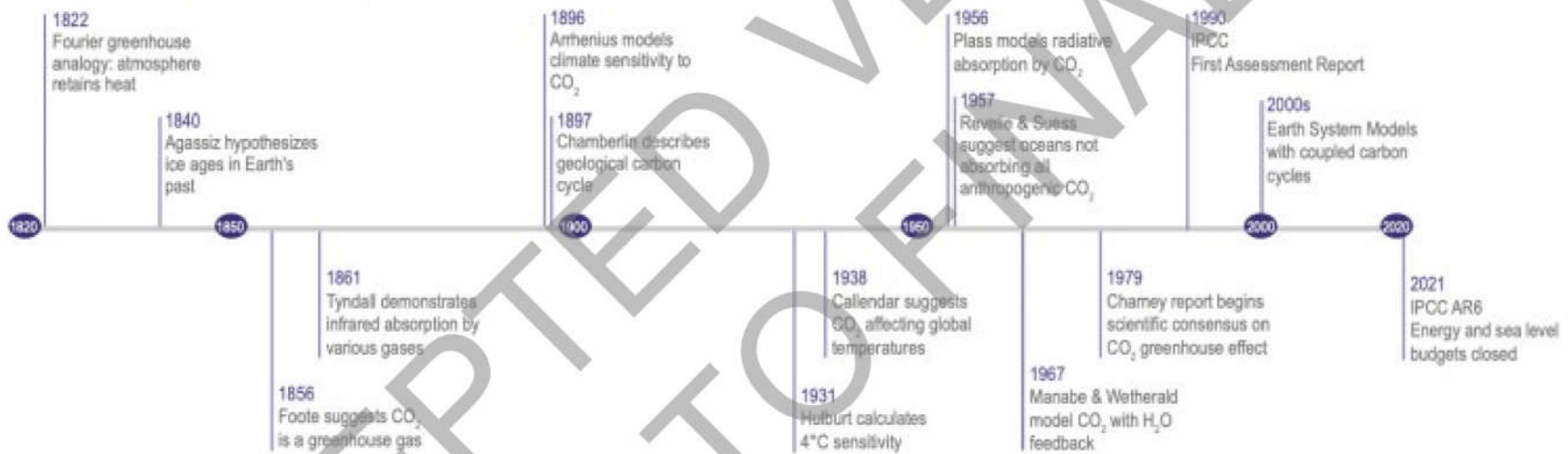


Observations





CO₂ and the enhanced greenhouse effect



Changes are occurring throughout the climate system

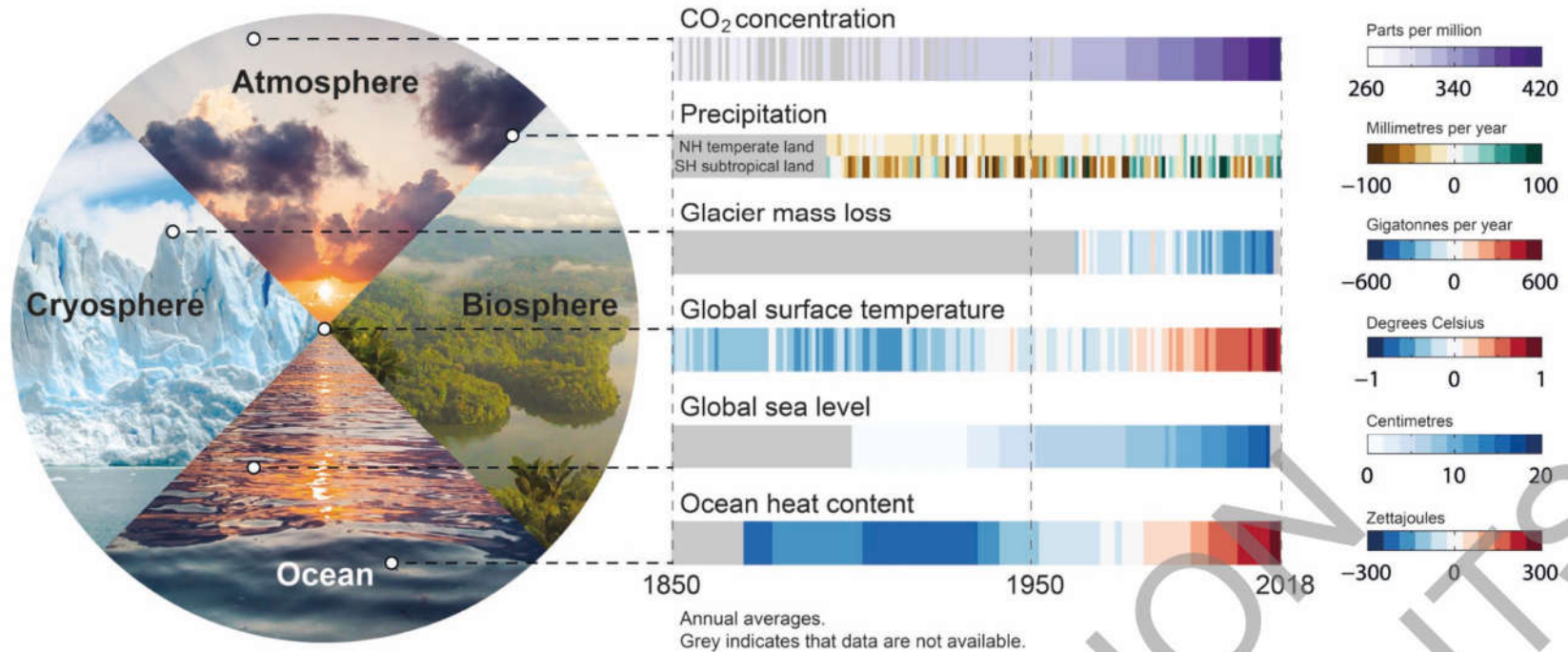


Figure 1.4: Changes are occurring throughout the climate system. Left: Main realms of the climate system:

Figure 1.4: Changes are occurring throughout the climate system. Left: Main realms of the climate system: atmosphere, biosphere, cryosphere, and ocean. Right: Six key indicators of ongoing changes since 1850, or the start of the observational or assessed record, through 2018. Each stripe indicates the global (except for precipitation which shows two latitude band means), annual mean anomaly for a single year, relative to a multi-year baseline (except for CO₂ concentration and glacier mass loss, which are absolute values). Grey indicates that data are not available. Datasets and baselines used are: (1) CO₂: Antarctic ice cores (Lüthi et al., 2008; Bereiter et al., 2015) and direct air measurements (Tans and Keeling, 2020) (see Figure 1.5 for details); (2) precipitation: Global Precipitation Climatology Centre (GPCC) V8 (updated from Becker et al. 2013), baseline 1961–1990 using land areas only with latitude bands 33°N–66°N and 15°S–30°S; (3) glacier mass loss: Zemp et al., 2019; (4) global surface air temperature (GMST): HadCRUT5 (Morice et al., 2021); baseline 1961–1990; (5) sea level change: (Dangendorf et al., 2019), baseline 1900–1929; (6) ocean heat content (model-observation hybrid): Zanna et al., (2019), baseline 1961–1990. Further details on data sources and processing are available in the chapter data table (Table 1.1).

IPCC 2021, Chap. 1

Klimaänderung I

2. Das sich verändernde Klimasystem

Robert Sausen

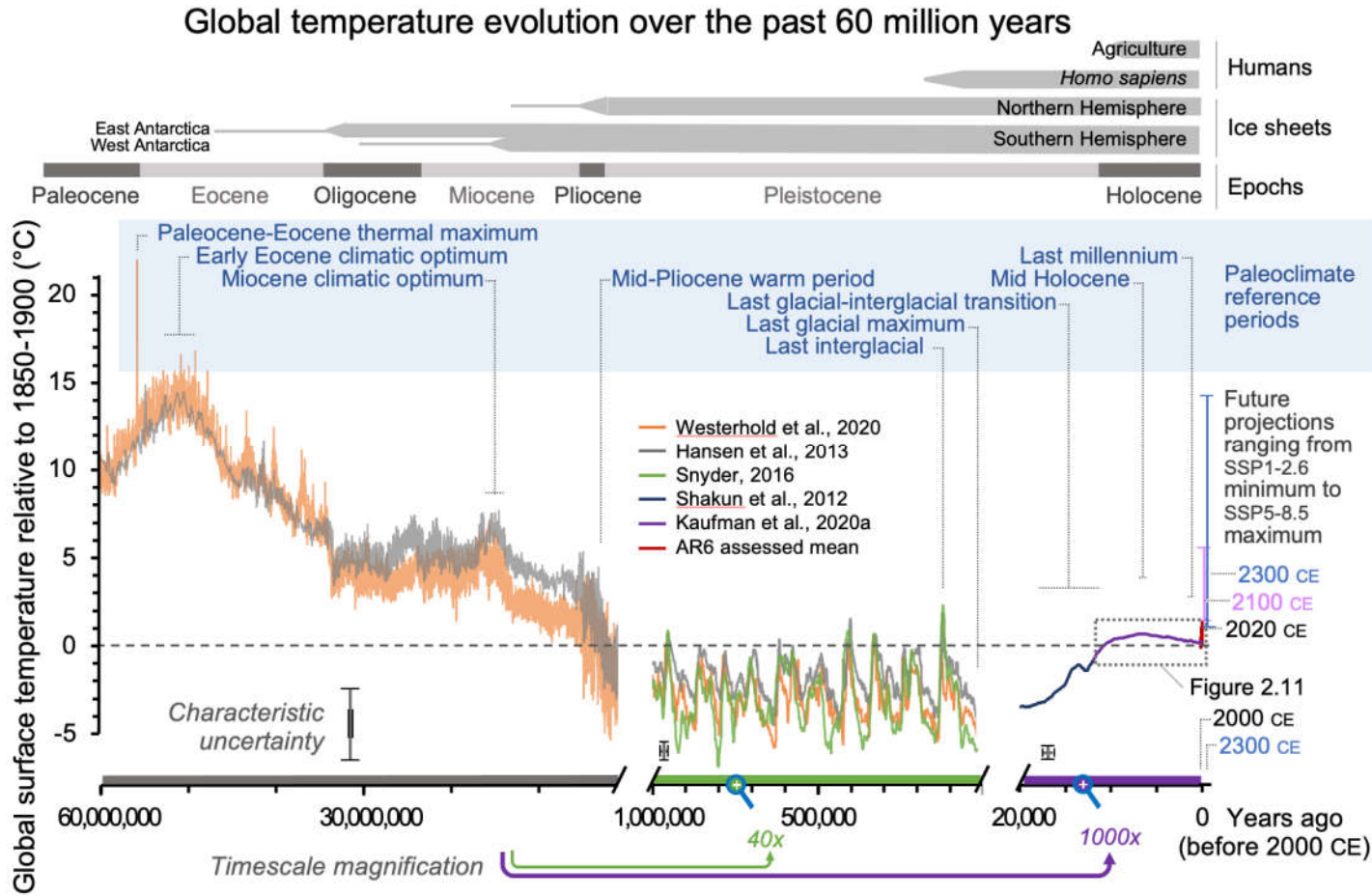
Institut für Physik der Atmosphäre
Deutsches Zentrum für Luft- und Raumfahrt
Oberpfaffenhofen

Vorlesung WS 2021/22

LMU München

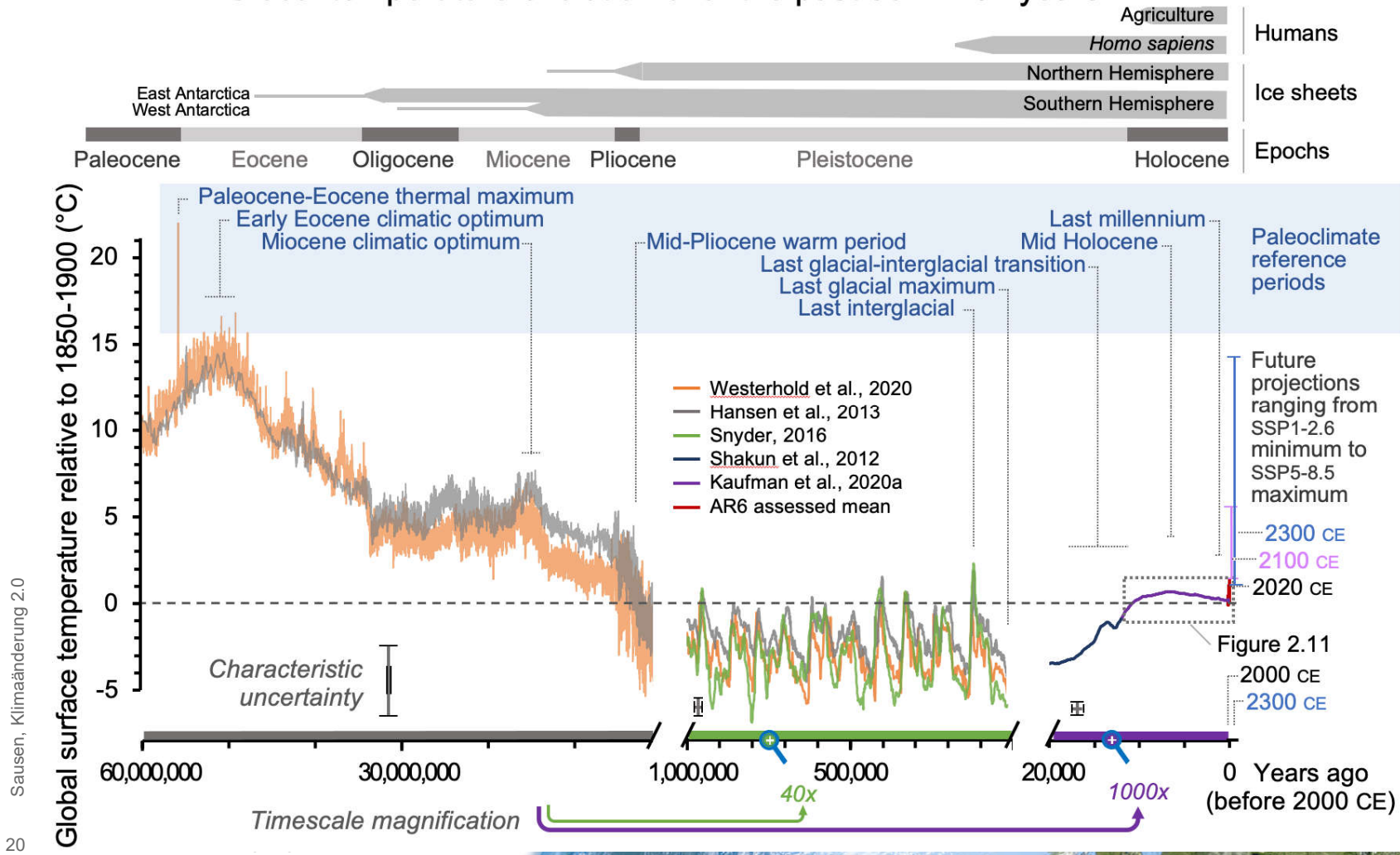


Knowledge for Tomorrow



Cross-Chapter Box 2.1, Figure 1: Global mean surface temperature (GMST) over the past 60 million years relative to 1850–1900 shown on three time scales. Information about each of the nine paleo reference periods (blue font) and sections in AR6 that discuss these periods are listed in Cross-Chapter Box 2.1 Table 1. Grey horizontal bars at the top mark important events. Characteristic uncertainties are based on expert judgement and are representative of the approximate midpoint of their respective time scales; uncertainties decrease forward in time. GMST estimates for most paleo reference periods (Figure 2.34) overlap with this reconstruction, but take into account multiple lines of evidence. Future projections span the range of global surface air temperature best estimates for SSP1–2.6 and SSP5–8.5 scenarios described in Section 1.6. Range shown for 2100 is based on CMIP6 multi-model mean for 2081–2100 from Table 4.5; range for 2300 is based upon an emulator and taken from Table 4.9. Further details on data sources and processing are available in the chapter data table (Table 2.SM.1).

Global temperature evolution over the past 60 million years



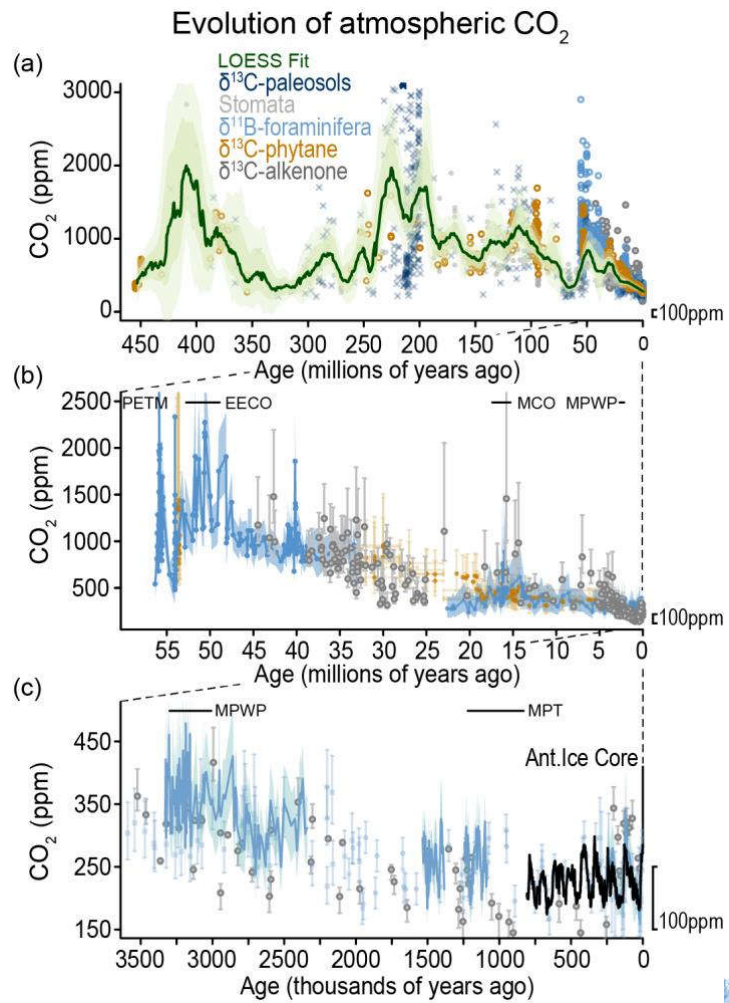
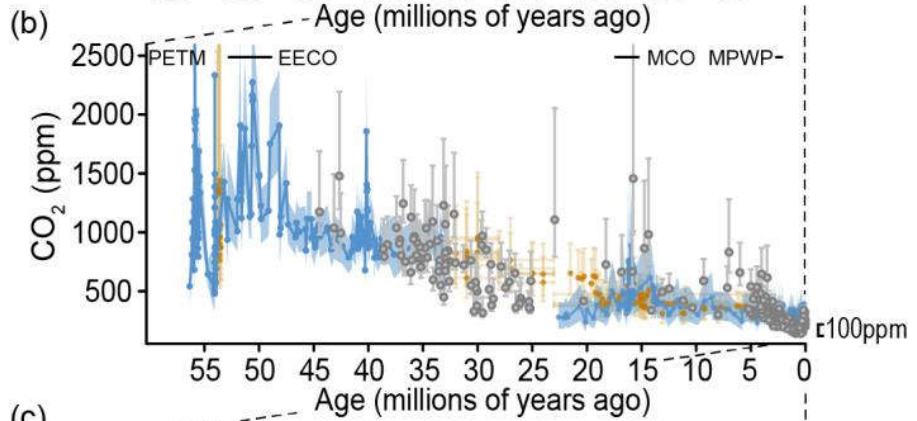
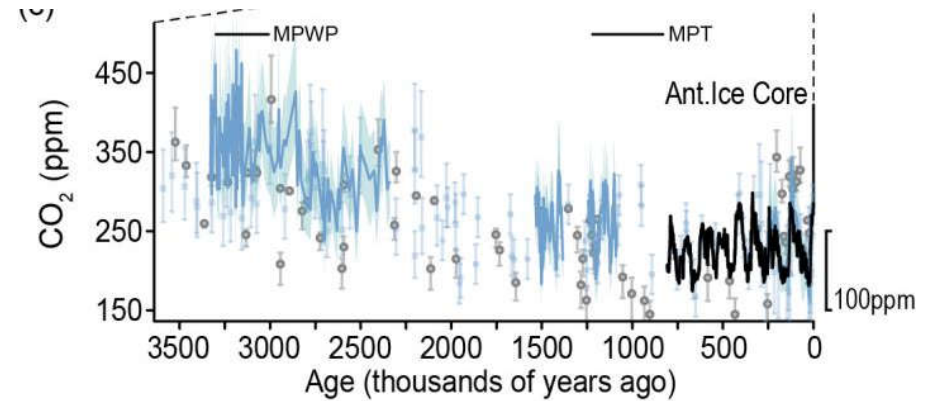
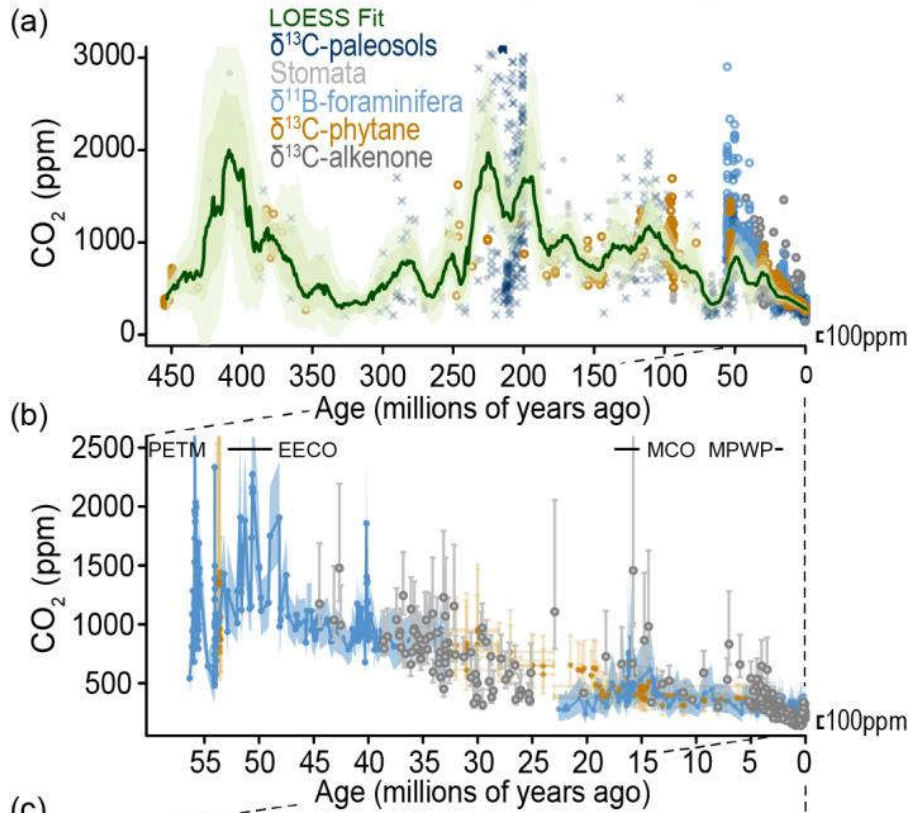


Figure 2.3: The evolution of atmospheric CO₂ through the last 450 million years. The periods covered are 0–450 Ma (a), 0–58 Ma (b), and 0–3500 ka (c), reconstructed from continental rock, marine sediment and ice core records. Note different timescales and axes ranges in panels (a), (b) and (c). Dark and light green bands in (a) are uncertainty envelopes at 68% and 95% uncertainty, respectively. 100 ppm in each panel is shown by the marker in the lower right hand corner to aid comparison between panels. In panel (b) and (c) the major paleoclimate reference periods (CCB2.1) have been labelled, and in addition: MPT (Mid Pleistocene Transition), MCO (Miocene Climatic Optimum). Further details on data sources and processing are available in the chapter data table (Table 2.SM.1).

Evolution of atmospheric CO₂

Evolution of atmospheric CO₂



Atmospheric WMGHG concentrations from ice cores

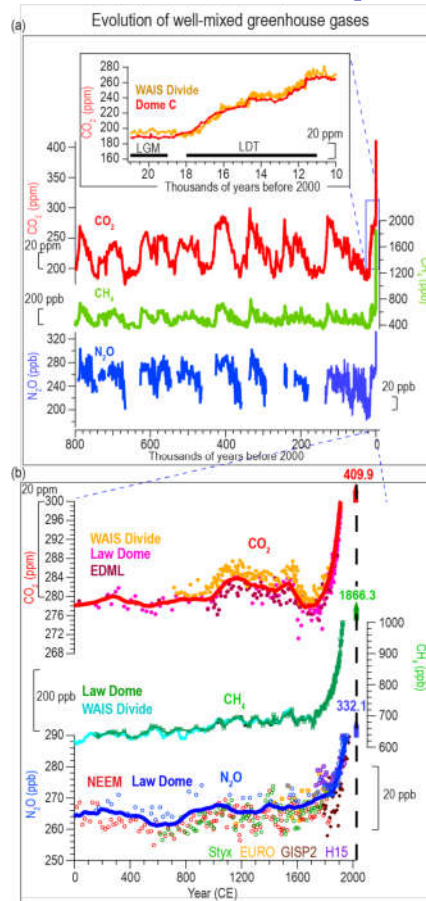
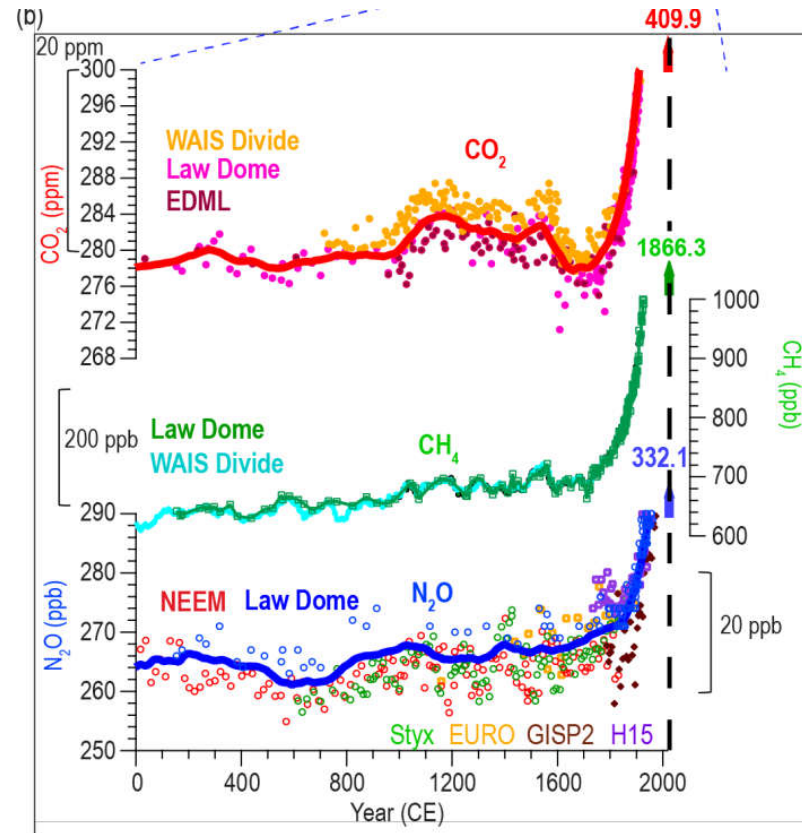
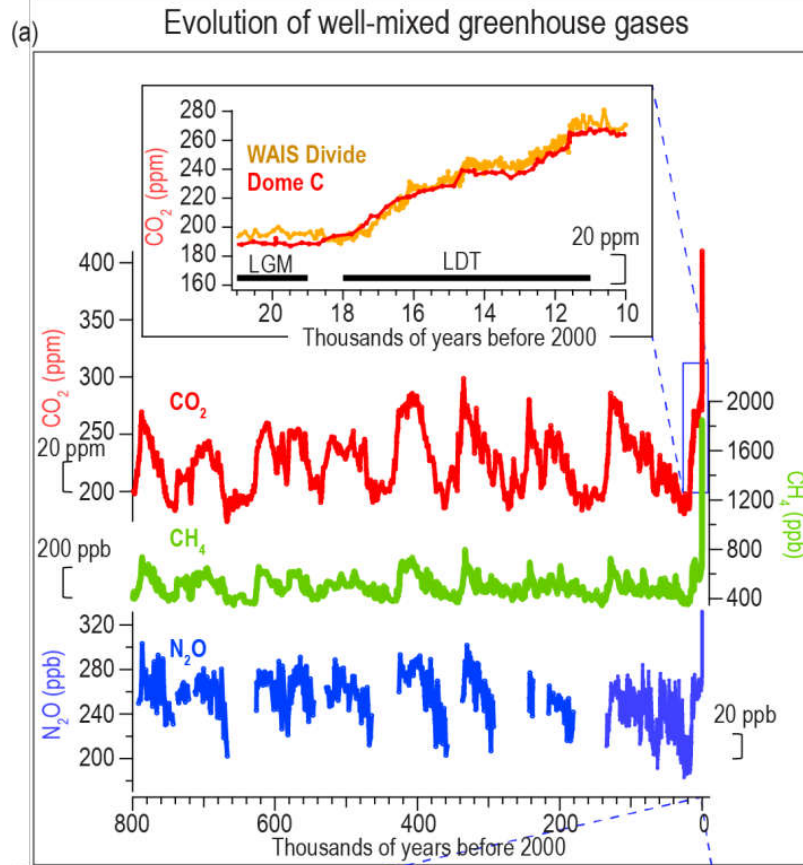


Figure 2.4: Atmospheric WMGHG concentrations from ice cores. (a) Records during the last 800 kyr with the LGM to Holocene transition as inset. (b) Multiple high-resolution records over the CE. The horizontal black bars in the panel a inset indicate Last Glacial Maximum (LGM) and Last Deglacial Termination (LDT) respectively. The red and blue lines in (b) are 100-year running averages for CO₂ and N₂O concentrations, respectively. The numbers with vertical arrows in (b) are instrumentally measured concentrations in 2019. Further details on data sources and processing are available in the chapter data table (Table 2.SM.1).



Atmospheric WMGHG concentrations from ice cores



Globally averaged dry-air mole fractions of greenhouse gases

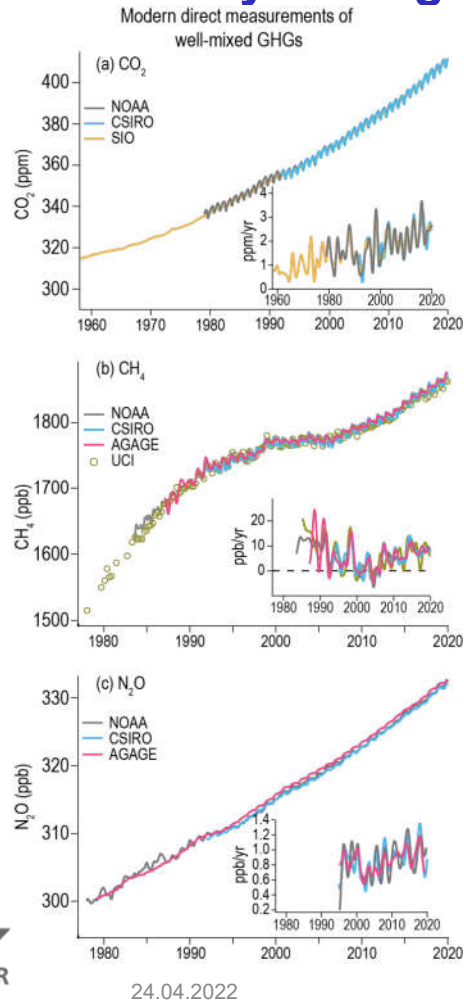
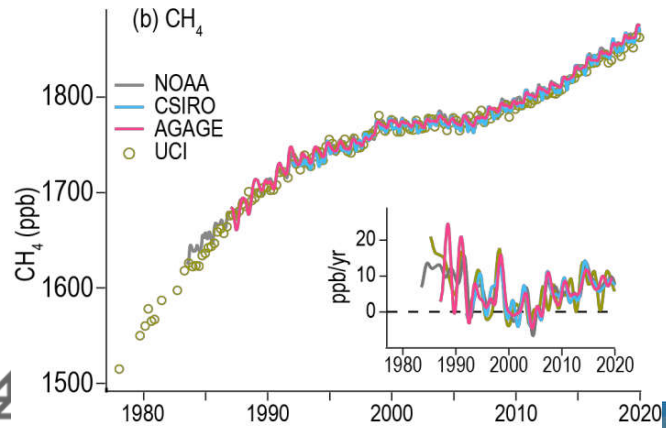
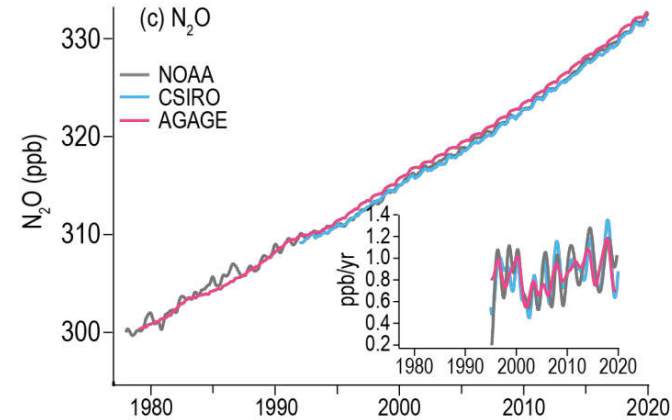
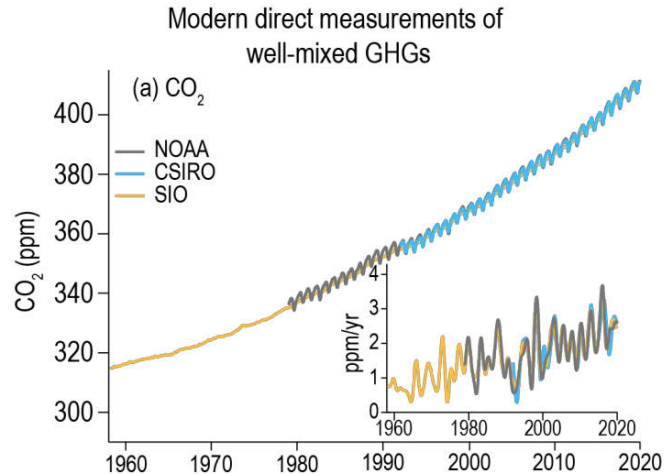


Figure 2.5: Globally averaged dry-air mole fractions of greenhouse gases. (a) CO₂ from SIO, CSIRO, and NOAA/GML (b) CH₄ from NOAA, AGAGE, CSIRO, and UCI; and (c) N₂O from NOAA, AGAGE, and CSIRO (see Table 2.2). Growth rates, calculated as the time derivative of the global means after removing seasonal cycle are shown as inset figures. Note that the CO₂ series is 1958–2019 whereas CH₄, and N₂O are 1979–2019. Further details on data are in Annex III, and on data sources and processing are available in the chapter data table (Table 2.SM.1).



Globally averaged dry-air mole fractions of greenhouse gases

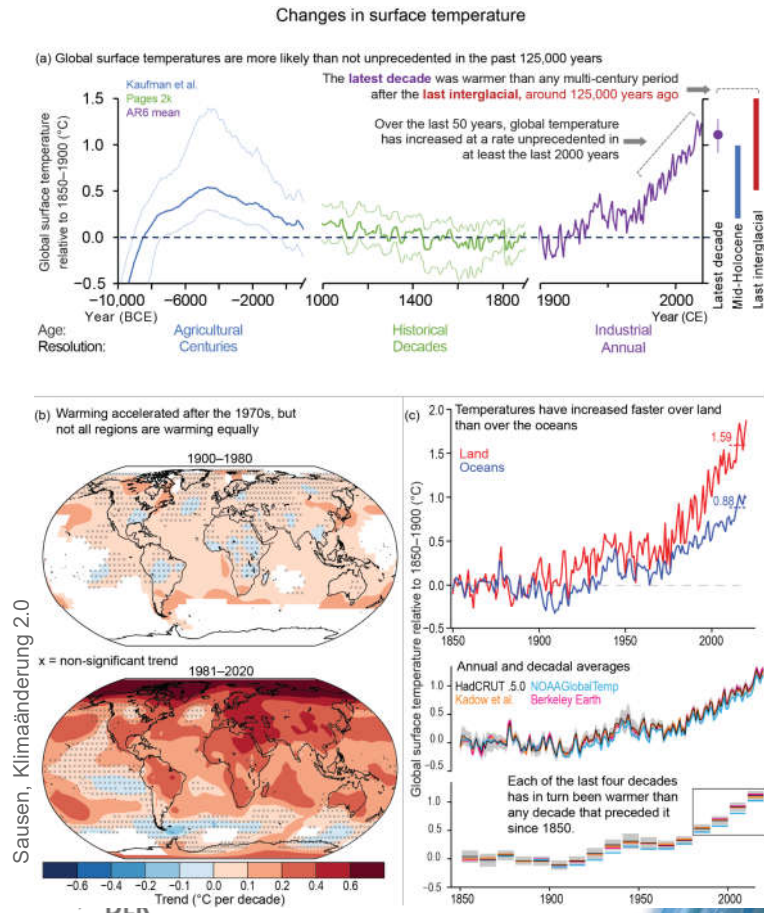


IPCC 2021, Chap. 2



Earth's surface temperature history

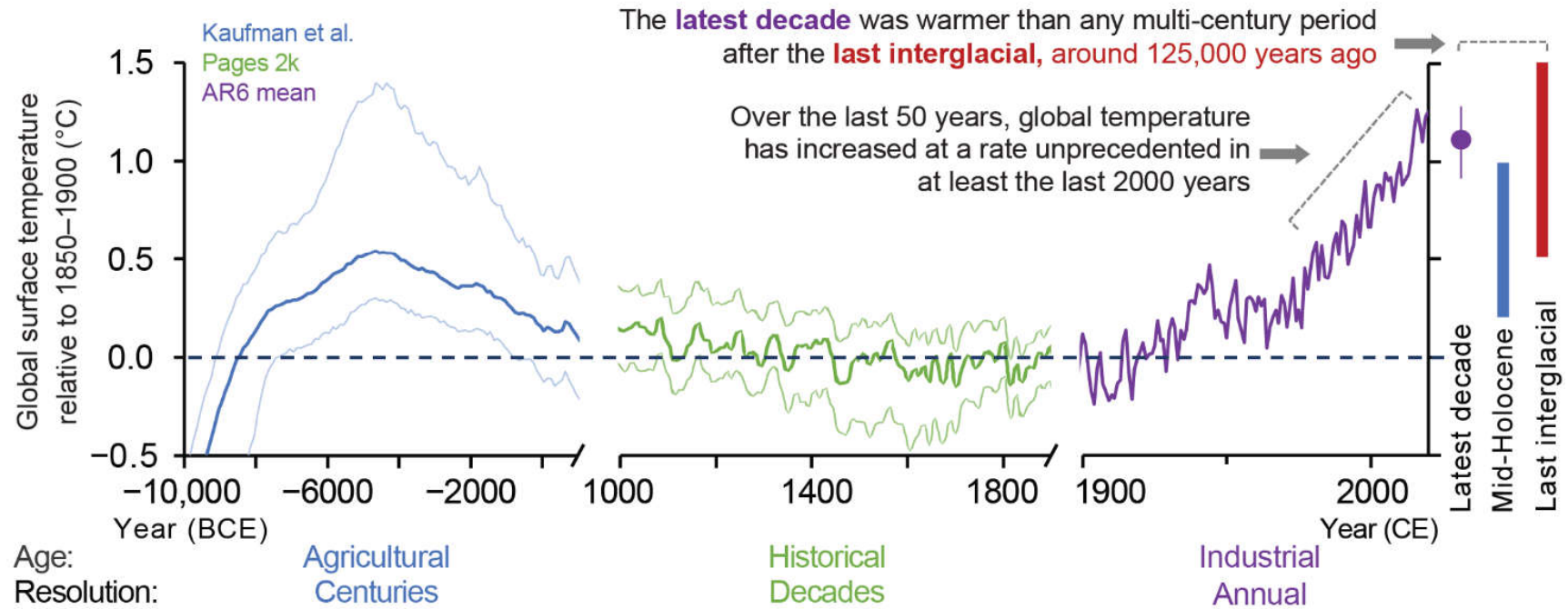
Figure 2.11: Earth's surface temperature history with key findings annotated within each panel. (a) GMST over the Holocene divided into three time scales. (i) 12 kyr–1 kyr in 100-year time steps, (ii) 1000–1900 CE, 10-year smooth, and (iii) 1900–2020 CE (from panel c). Median of the multi-method reconstruction (bold lines), with 5th and 95th percentiles of the ensemble members (thin lines). Vertical bars are the assessed *medium confidence* ranges of GMST for the Last Interglacial and mid-Holocene (Section 2.3.1.1). The last decade value and *very likely* range arises from 2.3.1.1.3. (b) Spatially resolved trends (°C per decade) for HadCRUTv5 over (upper map) 1900–1980, and (lower map) 1981–2020. 'x' marks denote non-significant trends. (c) Temperature from instrumental data for 1850–2020, including (upper panel) multi-product mean annual timeseries assessed in Section 2.3.1.1.3 for temperature over the oceans (blue line) and temperature over the land (red line) and indicating the warming to the most recent 10 years; and annually (middle panel) and decadal (bottom panel) resolved averages for the GMST datasets assessed in Section 2.3.1.1.3. The grey shading in each panel shows the uncertainty associated with the HadCRUT5 estimate (Morice et al., 2021). All temperatures relative to the 1850–1900 reference period. Further details on data sources and processing are available in the chapter data table (Table 2.SM.1).



Sausen, Klimaänderung 2.0

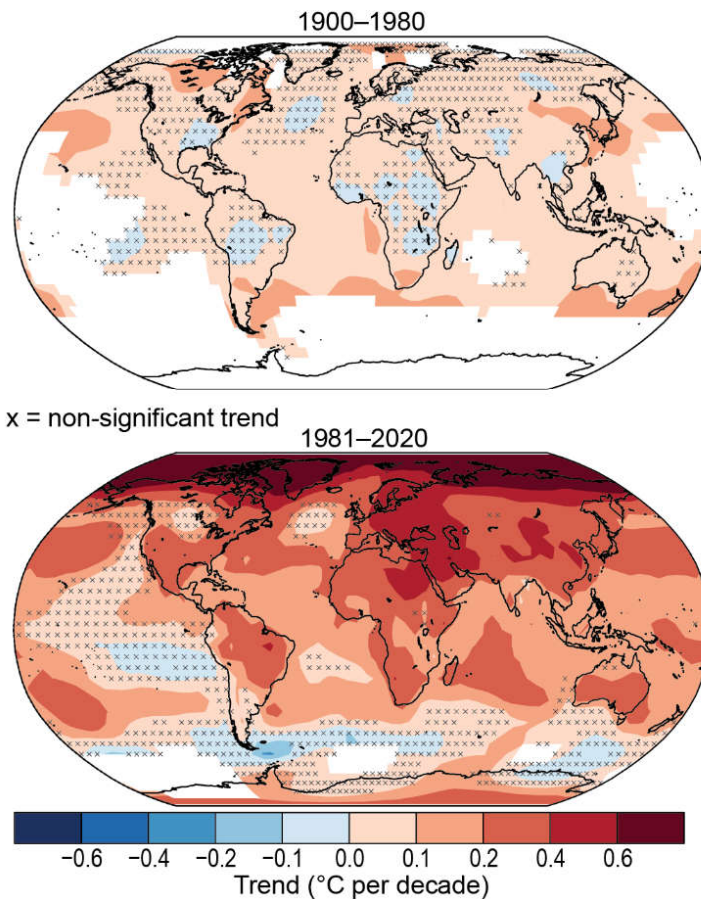
Changes in surface temperature

(a) Global surface temperatures are more likely than not unprecedented in the past 125,000 years



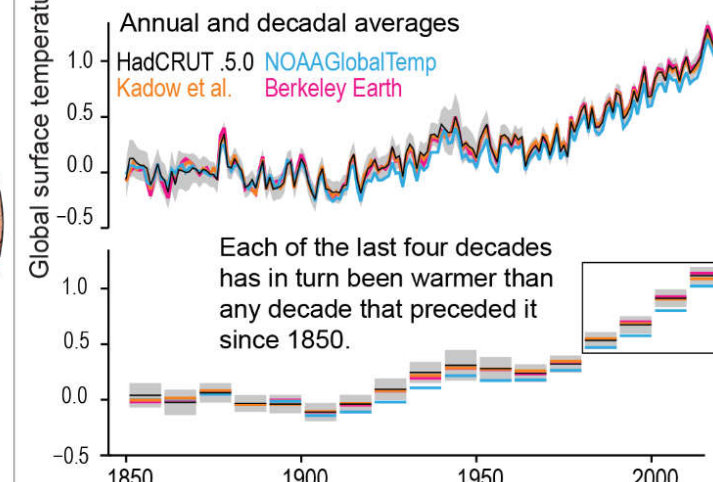
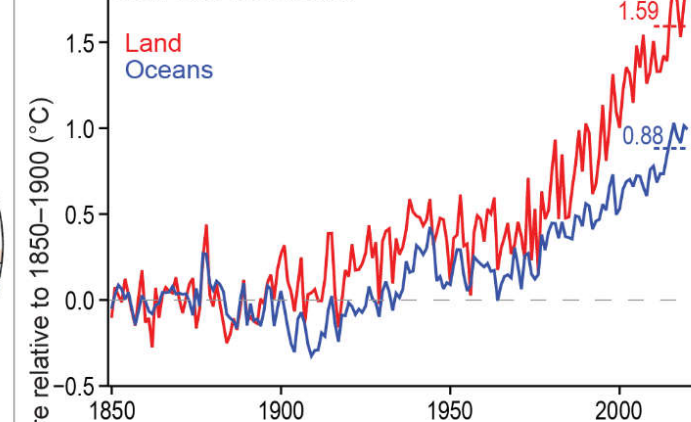


(b) Warming accelerated after the 1970s, but not all regions are warming equally



24.04.2022

(c) Temperatures have increased faster over land than over the oceans



Klimaänderung I

3. Der Einfluss des Menschen auf das Klimasystem

Robert Sausen

Institut für Physik der Atmosphäre
Deutsches Zentrum für Luft- und Raumfahrt
Oberpfaffenhofen

Vorlesung WS 2021/22

LMU München



Knowledge for Tomorrow

Statements in the Executive Summary

Synthesis across the Climate System (1)

It is unequivocal that human influence has warmed the global climate system since pre-industrial times. Combining the evidence from across the climate system increases the level of confidence in the attribution of observed climate change to human influence and reduces the uncertainties associated with assessments based on single variables. Large-scale indicators of climate change in the atmosphere, ocean, cryosphere and at the land surface show clear responses to human influence consistent with those expected based on model simulations and physical understanding. {3.8.1}



Observed and simulated time series of the anomalies in annual and global mean near-surface air temperature (GSAT)

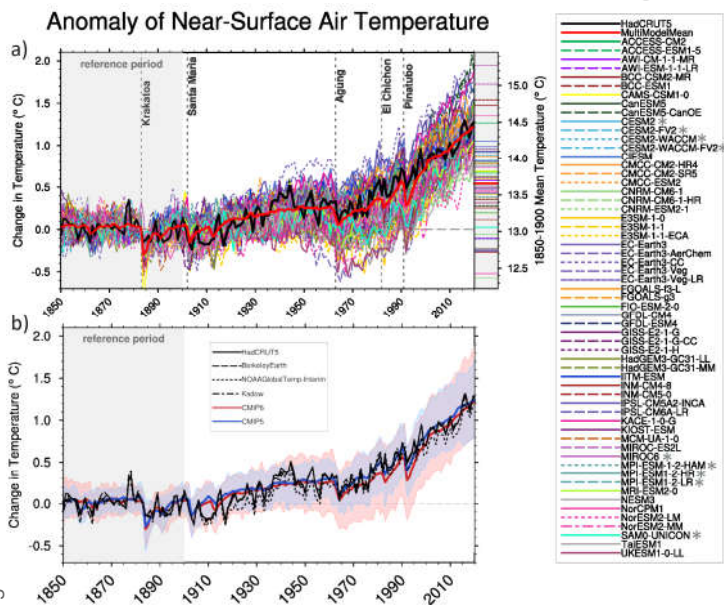
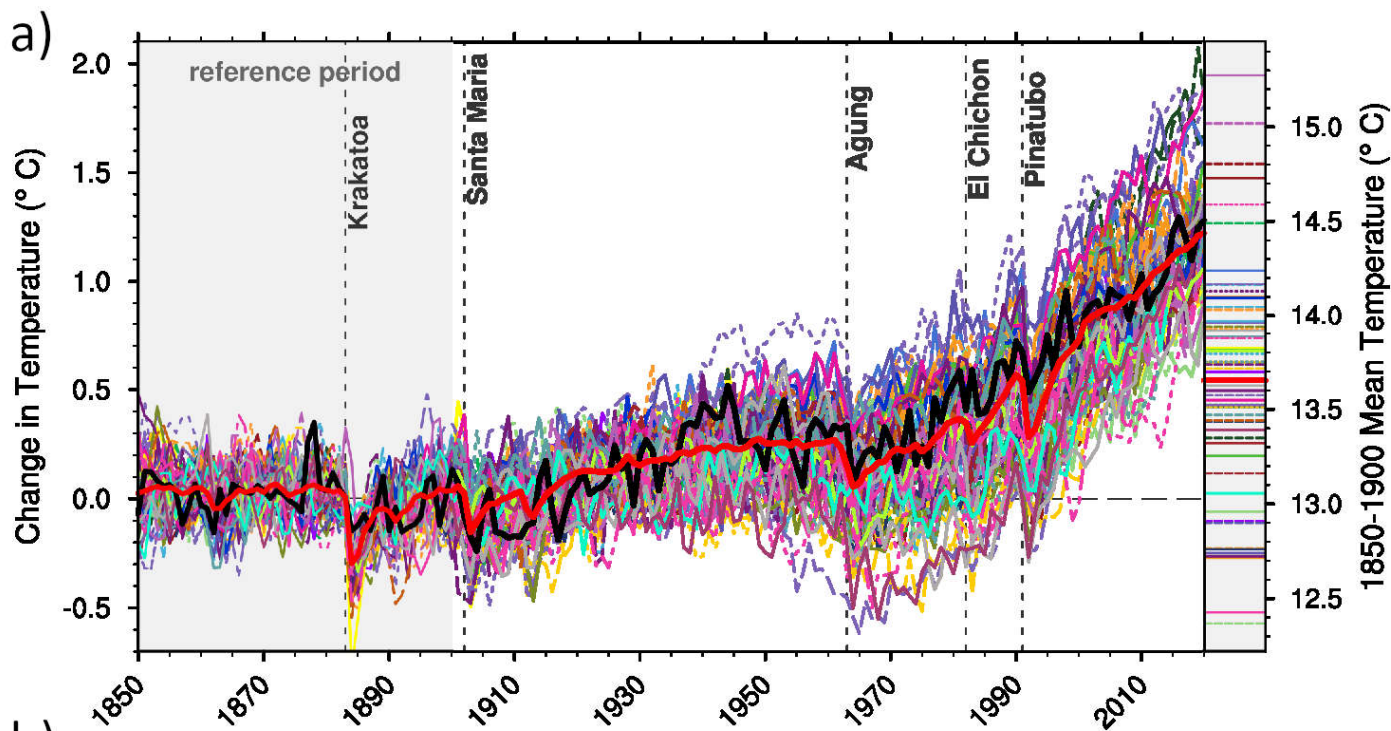


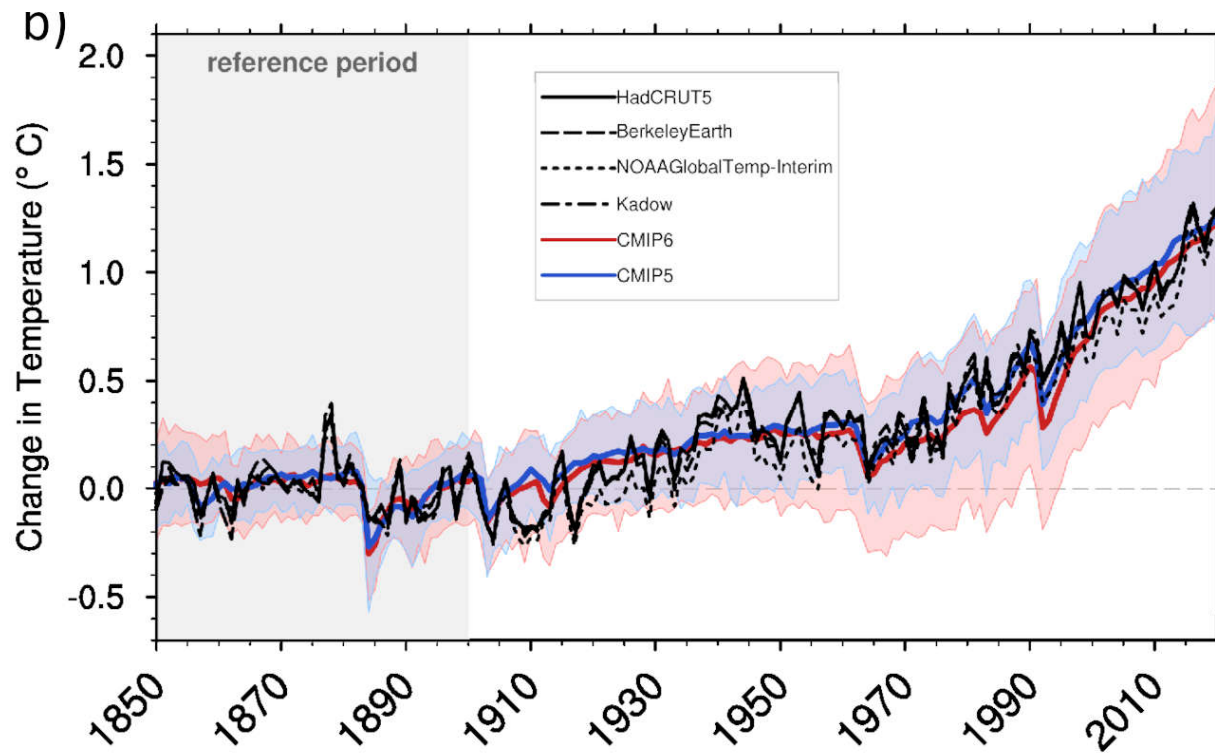
Figure 3.4: Observed and simulated time series of the anomalies in annual and global mean near-surface air temperature (GSAT). All anomalies are differences from the 1850–1900 time-mean of each individual time series. The reference period 1850–1900 is indicated by grey shading. (a) Single simulations from CMIP6 models (thin lines) and the multi-model mean (thick red line). Observational data (thick black lines) are HadCRUT5, and are blended surface temperature (2 m air temperature over land and sea surface temperature over the ocean). All models have been subsampled using the HadCRUT5 observational data mask. Vertical lines indicate large historical volcanic eruptions. CMIP6 models which are marked with an asterisk are either tuned to reproduce observed warming directly, or indirectly by tuning equilibrium climate sensitivity. Inset: GSAT for each model over the reference period, not masked to any observations. (b). Multi-model means of CMIP5 (blue line) and CMIP6 (red line) ensembles and associated 5 to 95 percentile ranges (shaded regions). Observational data are HadCRUT5, Berkeley Earth, NOAA Global Temp-Interim and Kadow et al. (2020). Masking was done as in (a). CMIP5 simulations are extended with SSP2-4.5 simulations for the period 2015–2020 and CMIP6 simulations are extended with RCP4.5 simulations for the period 2006–2020. All available ensemble members were used (see Section 3.2). The multi-model means and percentiles were calculated solely from simulations available for the whole time span (1850–2020). Figure is updated from Bock et al. (2020), their Figures 1 and 2. / CC BY4.0 <https://creativecommons.org/licenses/by/4.0/>. Further details on data sources and processing are available in the chapter data table (Table 3.SM.1).



Anomaly of Near-Surface Air Temperature



- HadCRUT5
- MultiModelMean
- ACCESS-CM2
- ACCESS-ESM1-5
- AWI-CM-1-1-MR
- AWI-ESM-1-1-LR
- BCC-CSM2-MR
- BCC-ESM1
- CAMS-CSM1-0
- CanESM5
- CanESM5-CanOE
- CESM2 *
- CESM2-FV2 *
- CESM2-WACCM*
- CESM2-WACCM-FV2*
- CIESM
- CMCC-CM2-HR4
- CMCC-CM2-SR5
- CMCC-ESM2
- CNRM-CM6-1
- CNRM-CM6-1-HR
- CNRM-ESM2-1
- E3SM-1-0
- E3SM-1-1
- E3SM-1-1-ECA
- EC-Earth3
- EC-Earth3-AerChem
- EC-Earth3-CC
- EC-Earth3-Veg
- EC-Earth3-Veg-LR
- FGOALS-f3-L
- FGOALS-g3
- FIO-ESM-2-0
- GFDL-CM4
- GFDL-ESM4
- GISS-E2-1-G
- GISS-E2-1-G-CC
- GISS-E2-1-H
- HadGEM3-GC31-LL
- HadGEM3-GC31-MM
- IITM-ESM
- INM-CM4-8
- INM-CM5-0
- IPSL-CM5A2-INCA
- IPSL-CM6A-LR
- KACE-1-0-G
- KIOST-ESM
- MCM-UA-1-0
- MIROC-ES2L
- MIROC6 *
- MPI-ESM-1-2-HAM *
- MPI-ESM1-2-HR *
- MPI-ESM1-2-LR *
- MRI-ESM2-0
- NESM3
- NorCPM1
- NorESM2-LM
- NorESM2-MM
- SAM0-UNICON *
- TaiESM1
- UKESM1-0-LL



- HadCRUT5
- MultiModelMean
- ACCESS-CM2
- ACCESS-ESM1-5
- AWI-CM-1-1-MR
- AWI-ESM-1-1-LR
- BCC-CSM2-MR
- BCC-ESM1
- CAMS-CSM1-0
- CanESM5
- CanESM5-CanOE
- CESM2 *
- CESM2-FV2 *
- CESM2-WACCM*
- CESM2-WACCM-FV2*
- CIESM
- CMCC-CM2-HR4
- CMCC-CM2-SR5
- CMCC-ESM2
- CNRM-CM6-1
- CNRM-CM6-1-HR
- CNRM-ESM2-1
- E3SM-1-0
- E3SM-1-1
- E3SM-1-1-ECA
- EC-Earth3
- EC-Earth3-AerChem
- EC-Earth3-CC
- EC-Earth3-Veg
- EC-Earth3-Veg-LR
- FGOALS-f3-L
- FGOALS-g3
- FIO-ESM-2-0
- GFDL-CM4
- GFDL-ESM4
- GISS-E2-1-G
- GISS-E2-1-G-CC
- GISS-E2-1-H
- HadGEM3-GC31-LL
- HadGEM3-GC31-MM
- IITM-ESM
- INM-CM4-8
- INM-CM5-0
- IPSL-CM5A2-INCA
- IPSL-CM6A-LR
- KACE-1-0-G
- KIOST-ESM
- MCM-UA-1-0
- MIROC-ES2L
- MIROC6 *
- MPI-ESM-1-2-HAM *
- MPI-ESM1-2-HR *
- MPI-ESM1-2-LR *
- MRI-ESM2-0
- NESM3
- NorCPM1
- NorESM2-LM
- NorESM2-MM
- SAM0-UNICON *
- TaiESM1
- UKESM1-0-LL



Assessed contributions to observed warming, and supporting lines of evidence

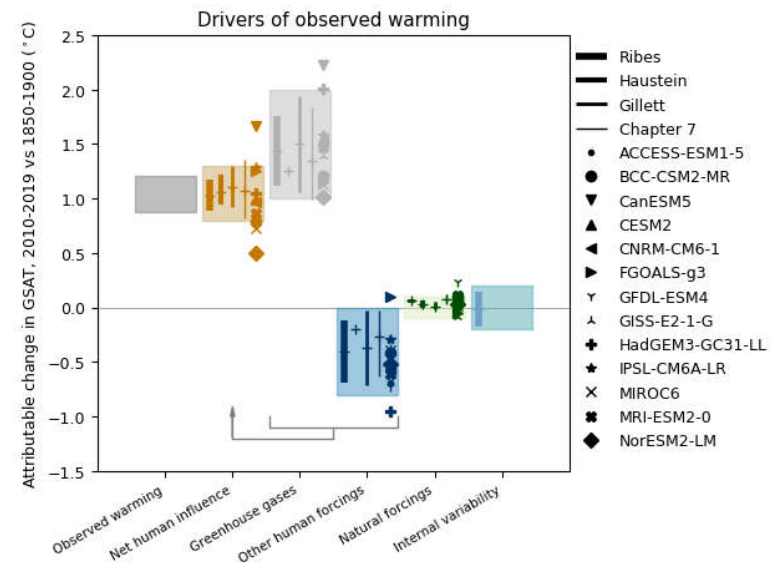
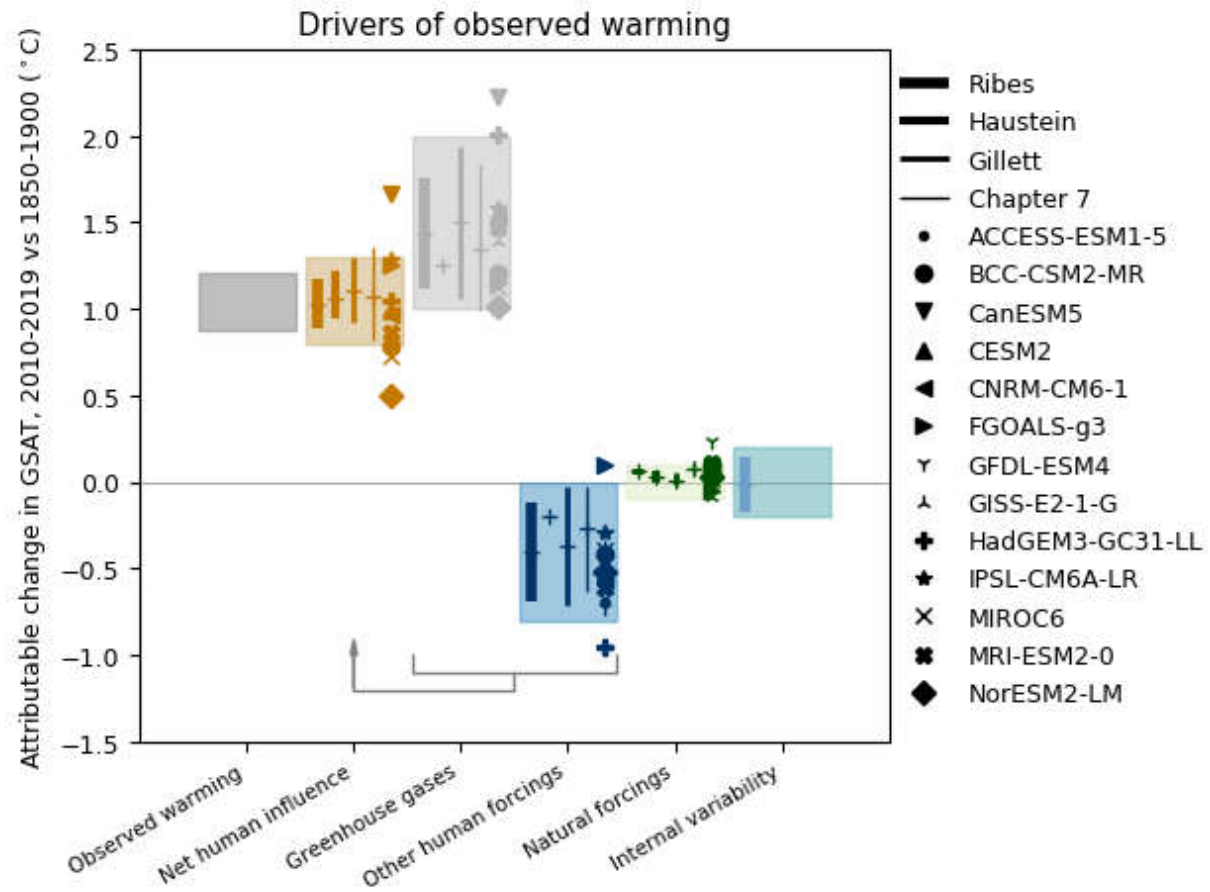


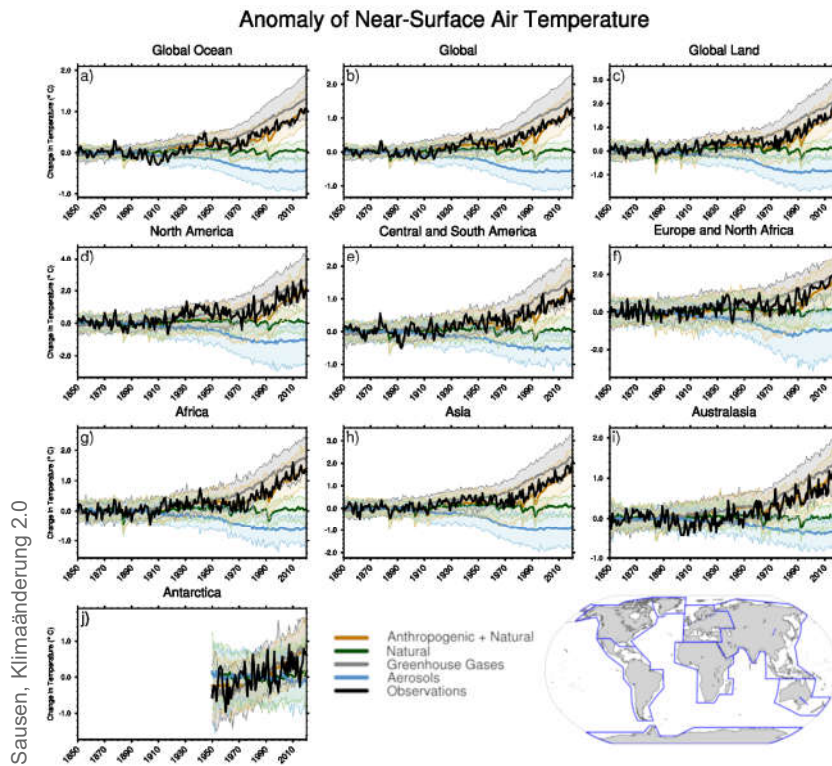
Figure 3.8: Assessed contributions to observed warming, and supporting lines of evidence. Shaded bands show assessed *likely* ranges of temperature change in GSAT, 2010-2019 relative to 1850-1900, attributable to net human influence, well-mixed greenhouse gases, other human forcings (aerosols, ozone, and land-use change), natural forcings, and internal variability, and the 5-95% range of observed warming. Bars show 5-95% ranges based on (left to right) Haustein et al. (2017), Gillett et al. (2021) and Ribes et al. (2021), and crosses show the associated best estimates. No 5-95% ranges were provided for the Haustein et al. (2017) greenhouse gas or other human forcings contributions. The Ribes et al. (2021) results were updated using a revised natural forcing time series, and the Haustein et al. (2017) results were updated using HadCRUT5. The Chapter 7 best estimates and ranges are derived using assessed forcing time series and a two-layer energy balance model as described in Section 7.3.5.3. Coloured symbols show the simulated responses to the forcings concerned in each of the models indicated. Further details on data sources and processing are available in the chapter data table (Table 3.SM.1).



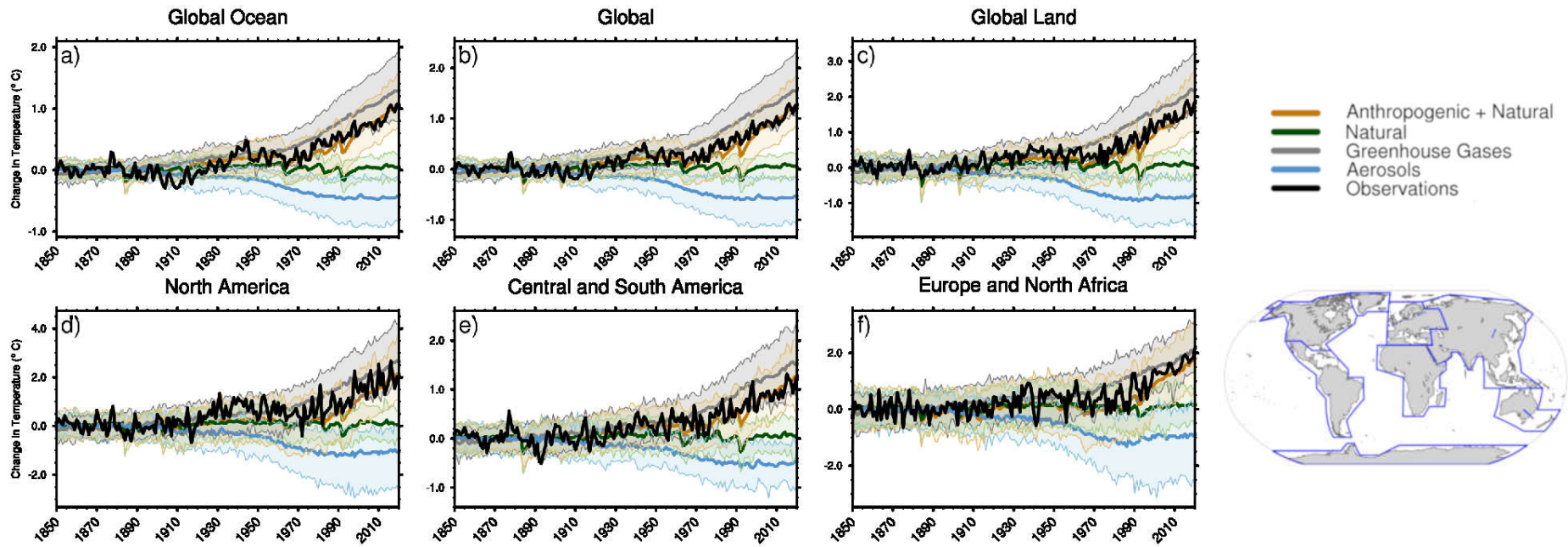


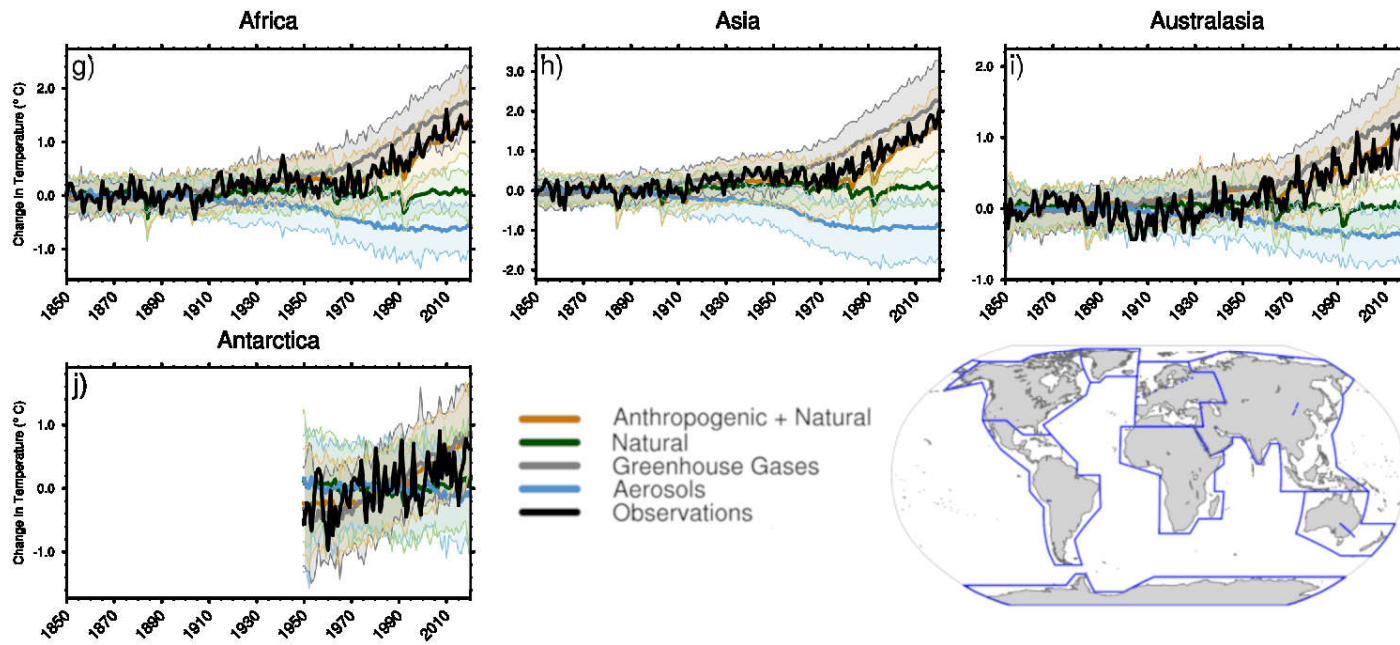
Global, land, ocean and continental annual mean near-surface air temperatures anomalies in CMIP6 models and observations

Figure 3.9: Global, land, ocean and continental annual mean near-surface air temperatures anomalies in CMIP6 models and observations. Time series are shown for CMIP6 historical anthropogenic and natural (brown), natural-only (green), greenhouse gas only (grey) and aerosol only (blue) simulations (multi-model means shown as thick lines, and shaded ranges between the 5th and 95th percentiles) and for HadCRUT5 (black). All models have been subsampled using the HadCRUT5 observational data mask. Temperatures anomalies are shown relative to 1950–2010 for Antarctica and relative to 1850–1900 for other continents. CMIP6 historical simulations are expanded by the SSP2-4.5 scenario simulations. All available ensemble members were used (see Section 3.2). Regions are defined by Iturbide et al. (2020). Further details on data sources and processing are available in the chapter data table (Table 3.SM.1).



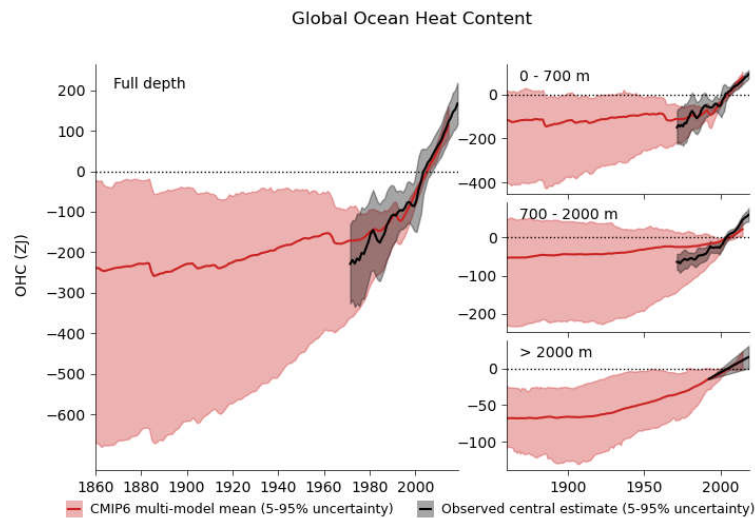
Anomaly of Near-Surface Air Temperature





Global ocean heat content in CMIP6 simulations and observations

Figure 3.26: Global ocean heat content in CMIP6 simulations and observations. Time series of observed (black) and simulated (red) global ocean heat content anomalies with respect to 1995-2014 for the full ocean depth (left panel), upper layer - 0 to 700 m (top right panel), intermediate layer -700 to 2000 m (middle right panel), and the abyssal ocean >2000 m (bottom right panel). The best estimate observations (black solid line) for the period of 1971-2018, along with *very likely* ranges (black shading) are from Section 2.3.3.1. For the models (1860-2014), ensemble members from 15 CMIP6 models are used to calculate the multi-model mean values (red solid line) after averaging across simulations for each independent model. The *very likely* ranges in the simulations are shown in red shading. Simulation drift has been removed from all CMIP6 historical runs using a contemporaneous portion of the linear fit to each corresponding pre-industrial control run (Gleckler et al., 2012). Units are 10^{21} Joules (Zettajoules). Further details on data sources and processing are available in the chapter data table (Table 3.SM.1).

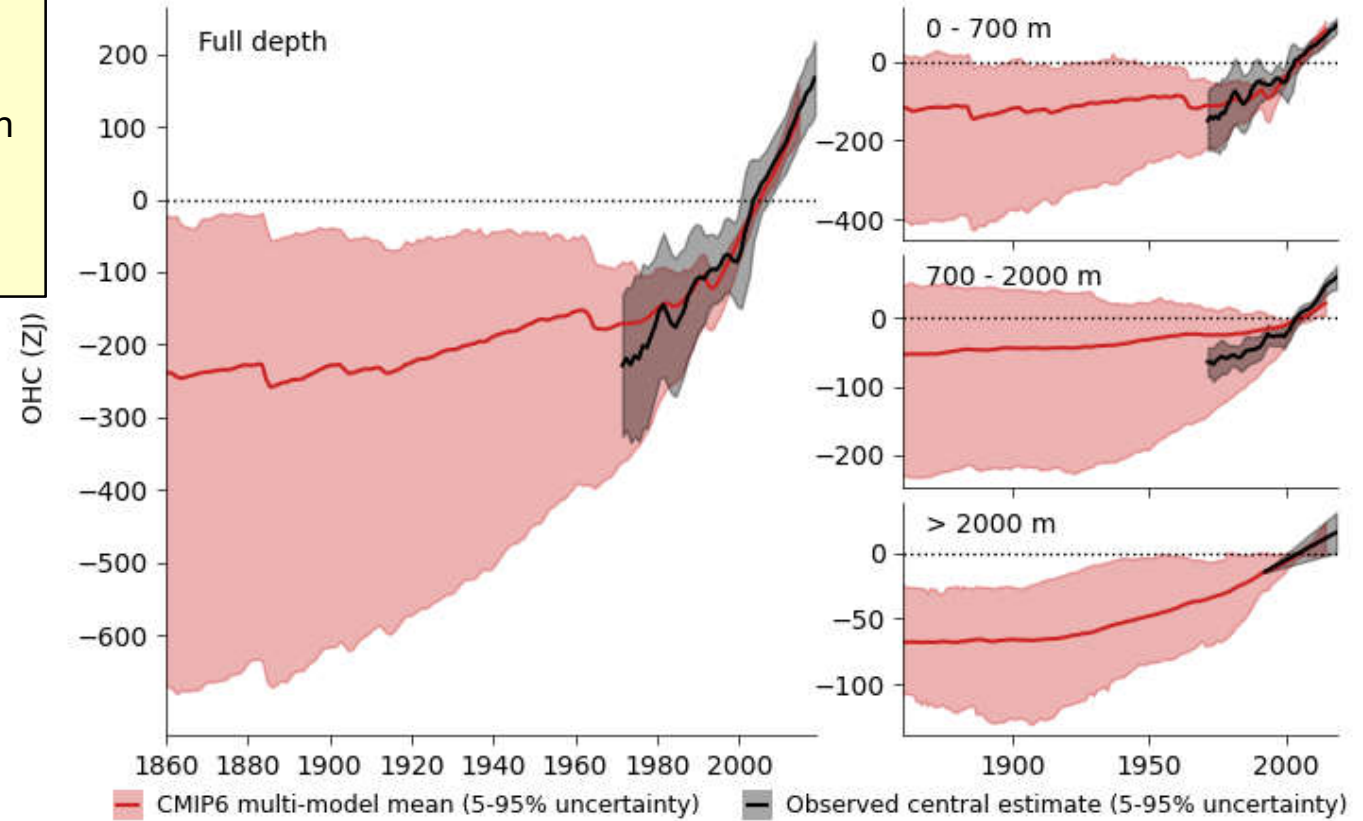


1 ZJ = 10^{21} J
 $\approx 2.78 \cdot 10^{11}$ kWh = 278 PWh

PV-Anlage Sausen: ~ 3.5 MWh

Windkraftanlage Berg:
 ~ 21 GWh (2021, 4 Turbinen)

Global Ocean Heat Content

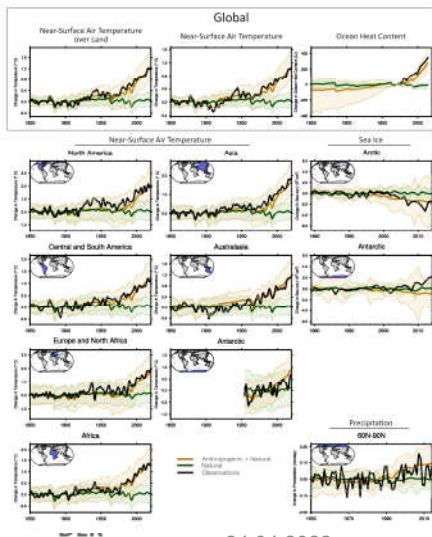


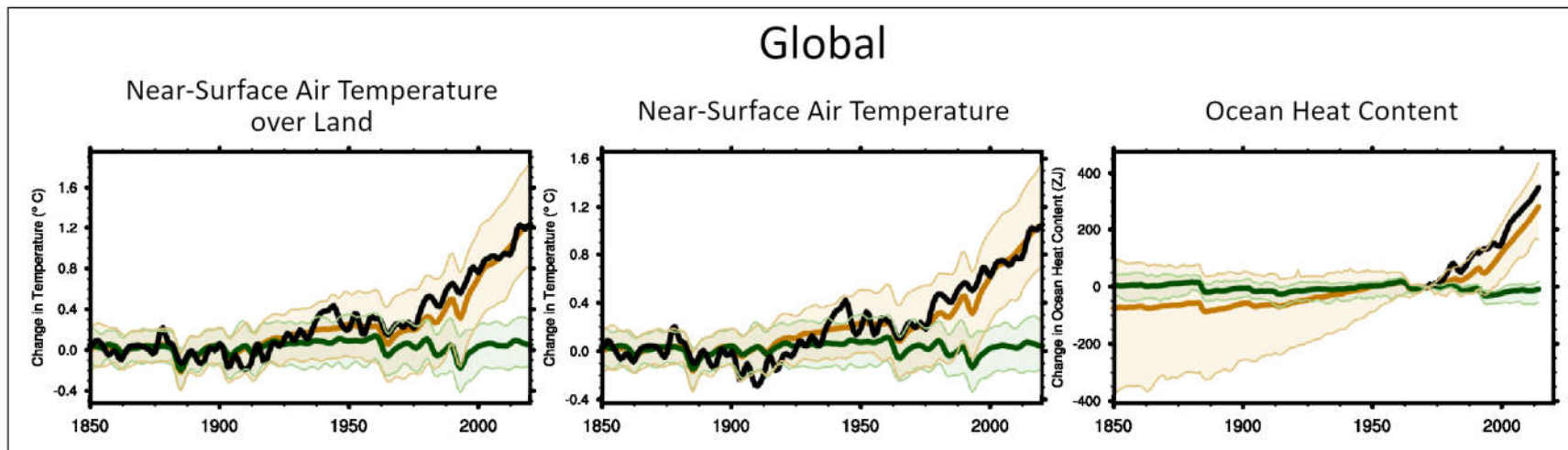
IPCC 2021, Chap. 3

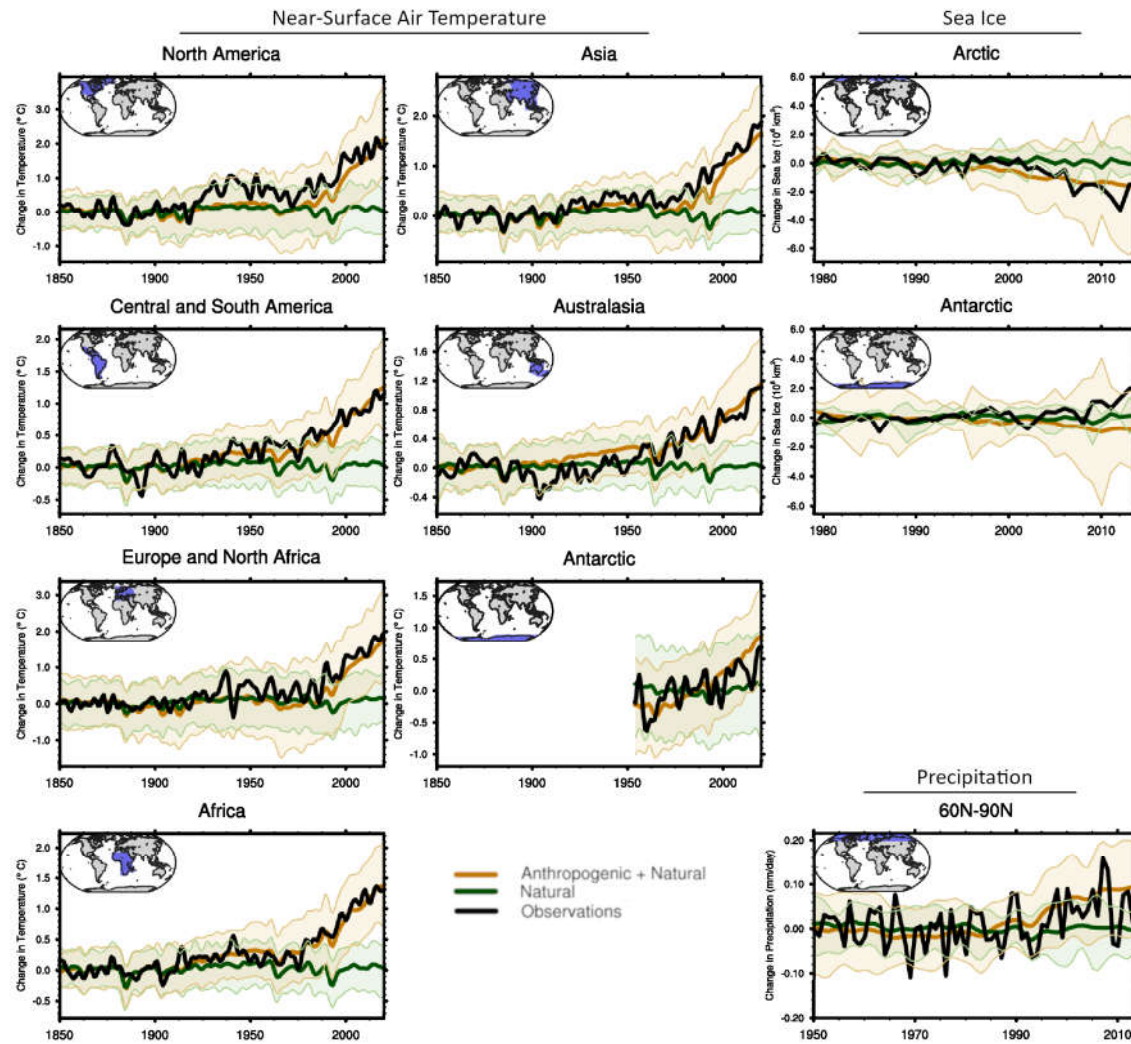


Summary figure showing simulated and observed changes in key large-scale indicators of climate change across the climate system

Figure 3.41: Summary figure showing simulated and observed changes in key large-scale indicators of climate change across the climate system, for continental, ocean basin and larger scales. Black lines show observations, brown lines and shading show the multi-model mean and 5th-95th percentile ranges for CMIP6 historical simulations including anthropogenic and natural forcing, and blue lines and shading show corresponding ensemble means and 5th-95th percentile ranges for CMIP6 natural-only simulations. Temperature time series are as in Figure 3.9, but with smoothing using a low pass filter. Precipitation time series are as in Figure 3.15 and ocean heat content as in Figure 3.26. Further details on data sources and processing are available in the chapter data table (Table 3.SM.1).







Klimaänderung I

4. Das zukünftige globale Klima: Szenarien-basierte Projektionen und kurzfristiger Ausblick

Robert Sausen

Institut für Physik der Atmosphäre
Deutsches Zentrum für Luft- und Raumfahrt
Oberpfaffenhofen

Vorlesung WS 2021/22

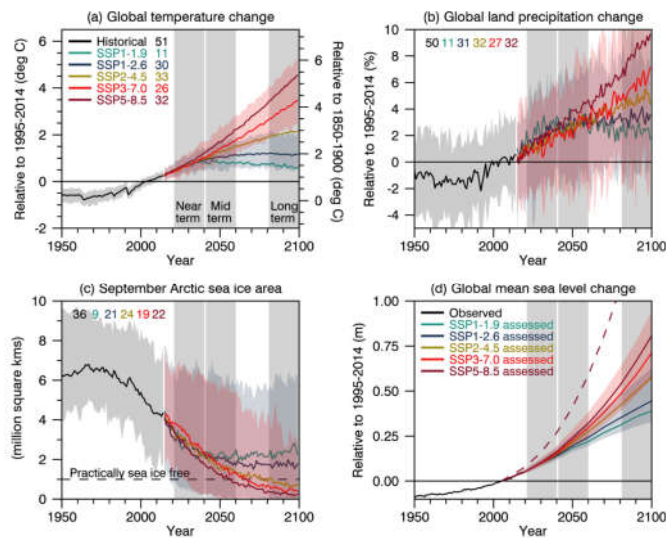
LMU München



Knowledge for Tomorrow

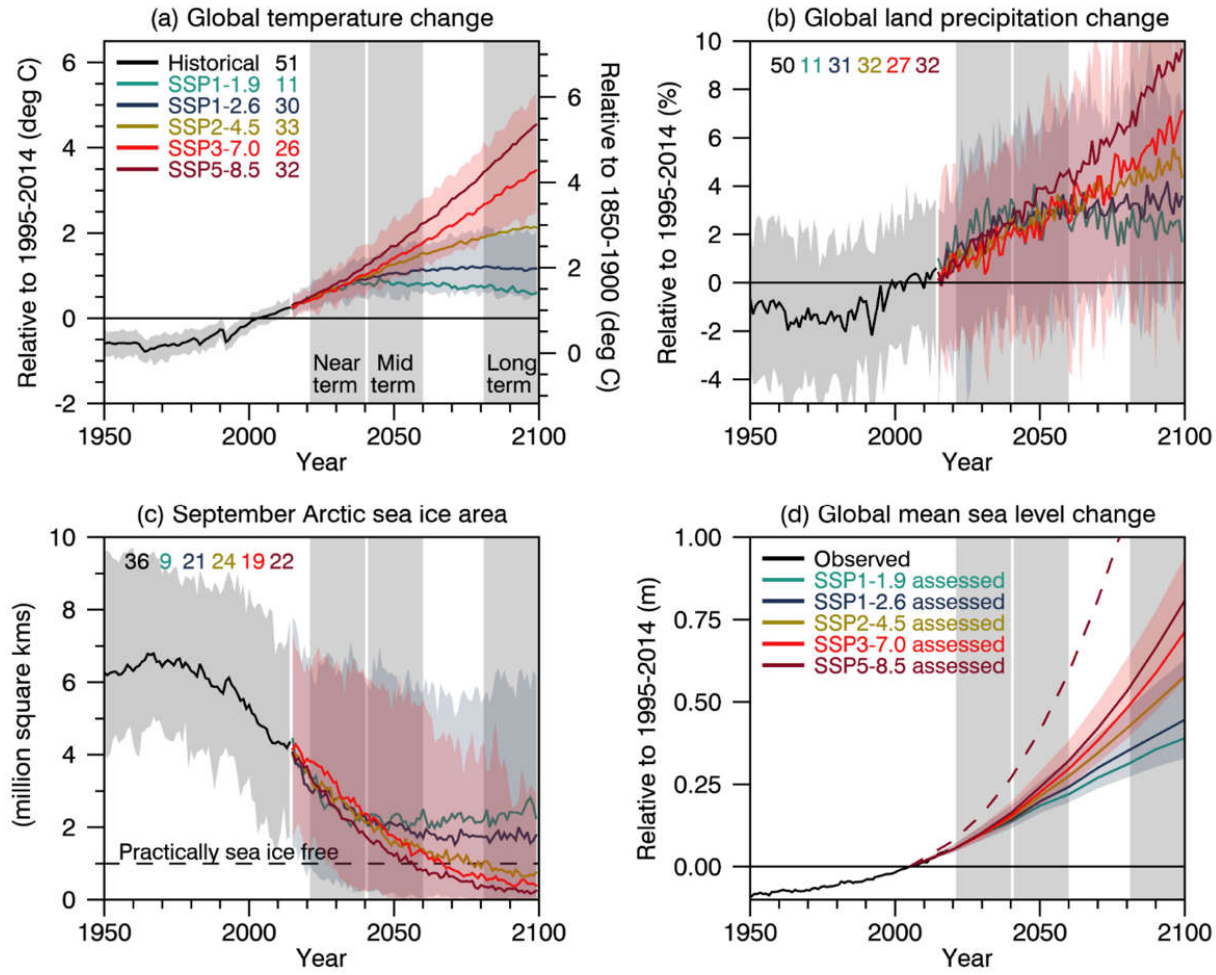
Selected indicators of global climate change from CMIP6 historical and scenario simulations

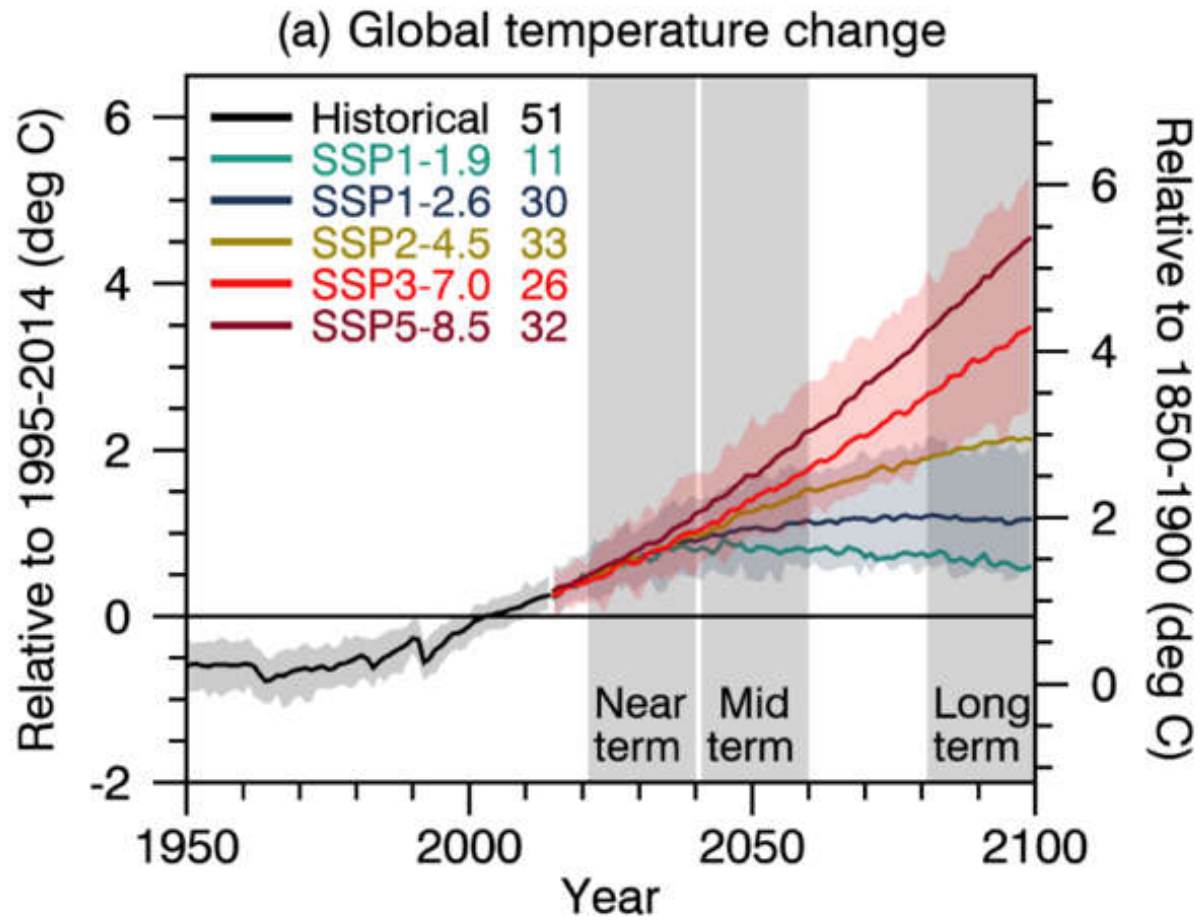
Figure 4.2: Selected indicators of global climate change from CMIP6 historical and scenario simulations. (a)



(b) Global land precipitation changes relative to the 1995–2014 average. (c) September Arctic sea-ice area. (d) Global mean sea-level change (GMSL) relative to the 1995–2014 average. (a), (b) and (d) are annual averages, (c) are September averages. In (a)-(c), the curves show averages over the CMIP6 simulations, the shadings around the SSP1-2.6 and SSP3-7.0 curves show 5–95% ranges, and the numbers near the top show the number of model simulations used. Results are derived from concentration-driven simulations. In (d), the barostatic contribution to GMSL (i.e., the contribution from land-ice melt) has been added offline to the CMIP6 simulated contributions from thermal expansion (thermosteric). The shadings around the SSP1-2.6 and SSP3-7.0 curves show 5–95% ranges. The dashed curve is the *low confidence* and low likelihood outcome at the high end of SSP5-8.5 and reflects deep uncertainties arising from potential ice-sheet and ice-cliff instabilities. This curve at year 2100 indicates 1.7 m of GMSL rise relative to 1995–2014. More information on the calculation of GMSL are available in Chapter 9, and further regional details are provided in the Atlas. Further details on data sources and processing are available in the chapter data table (Table 4.SM.1).

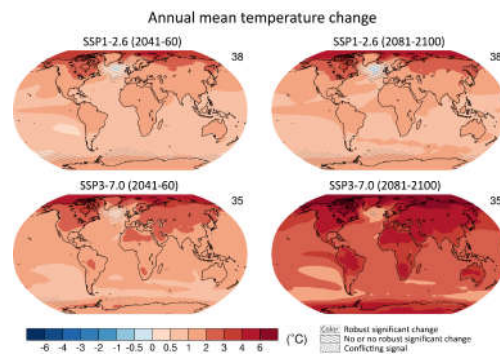






Mid- and long-term change of annual mean surface temperature

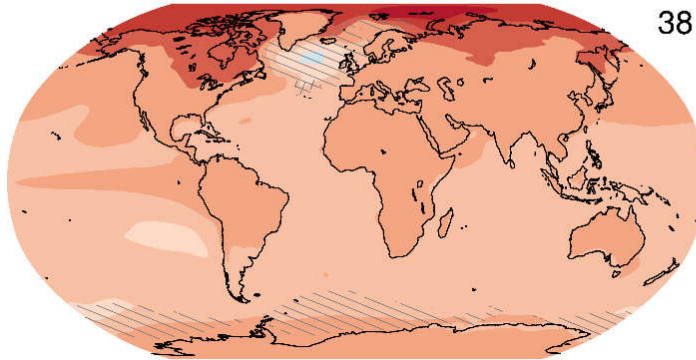
Figure 4.19: Mid- and long-term change of annual mean surface temperature. Displayed are projected spatial patterns of multi-model mean change in annual mean near-surface air temperature (°C) in 2041–2060 and 2081–2100 relative to 1995–2014 for (top) SSP1-2.6 and (bottom) SSP3-7.0. The number of models used is indicated in the top right of the maps. No overlay indicates regions where the change is robust and *likely* emerges from internal variability, that is, where at least 66% of the models show a change greater than the internal-variability threshold (see Section 4.2.6) and at least 80% of the models agree on the sign of change. Diagonal lines indicate regions with no change or no robust significant change, where fewer than 66% of the models show change greater than the internal-variability threshold. Crossed lines indicate areas of conflicting signals where at least 66% of the models show change greater than the internal-variability threshold but fewer than 80% of all models agree on the sign of change. Further details on data sources and processing are available in the chapter data table (Table 4.SM.1).



Annual mean temperature change

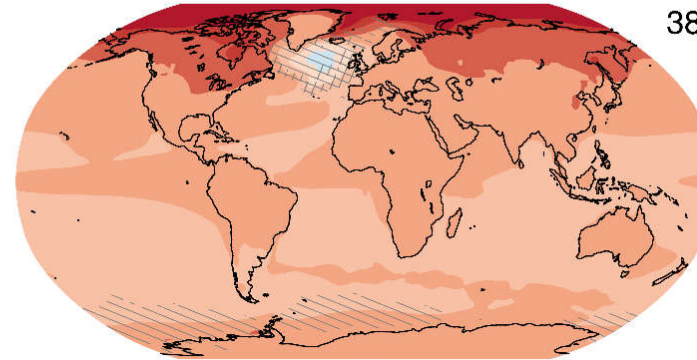
SSP1-2.6 (2041-60)

38



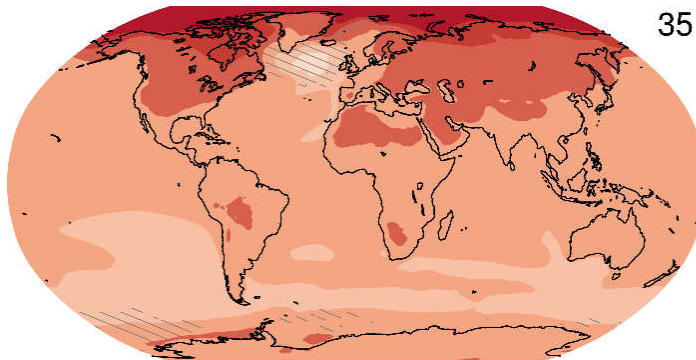
SSP1-2.6 (2081-2100)

38



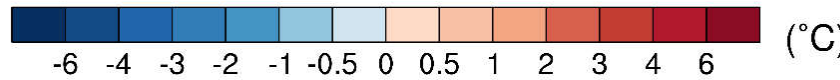
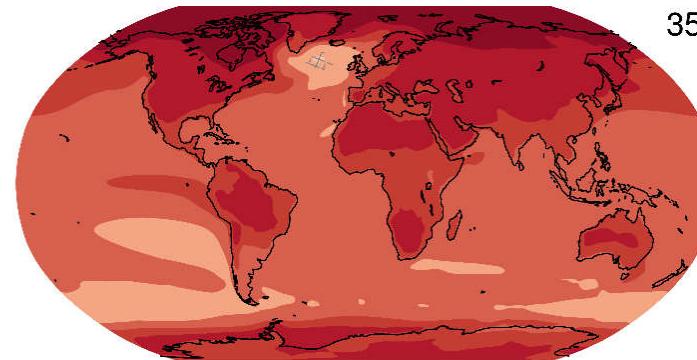
SSP3-7.0 (2041-60)

35



SSP3-7.0 (2081-2100)

35

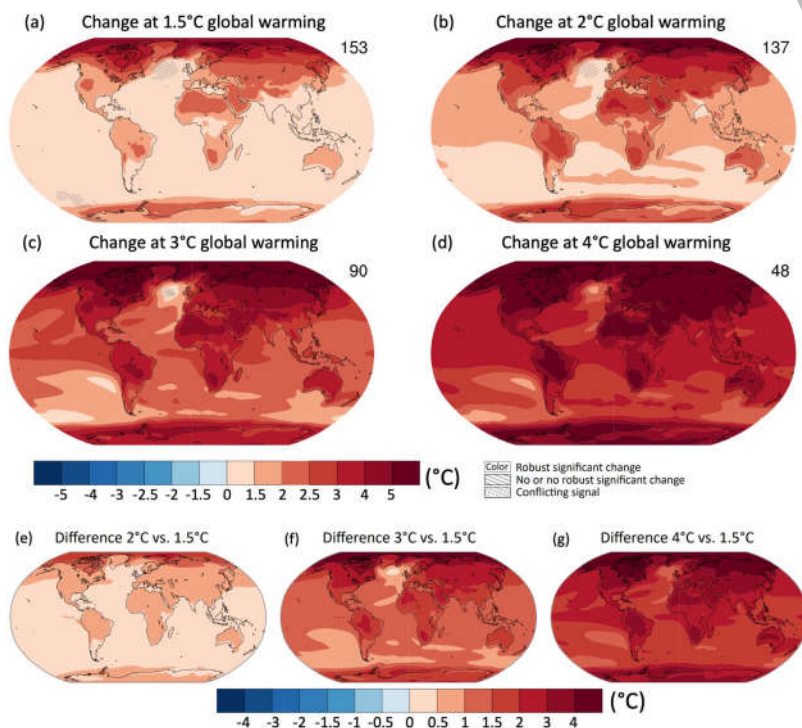


- Robust significant change
- No or no robust significant change
- Conflicting signal

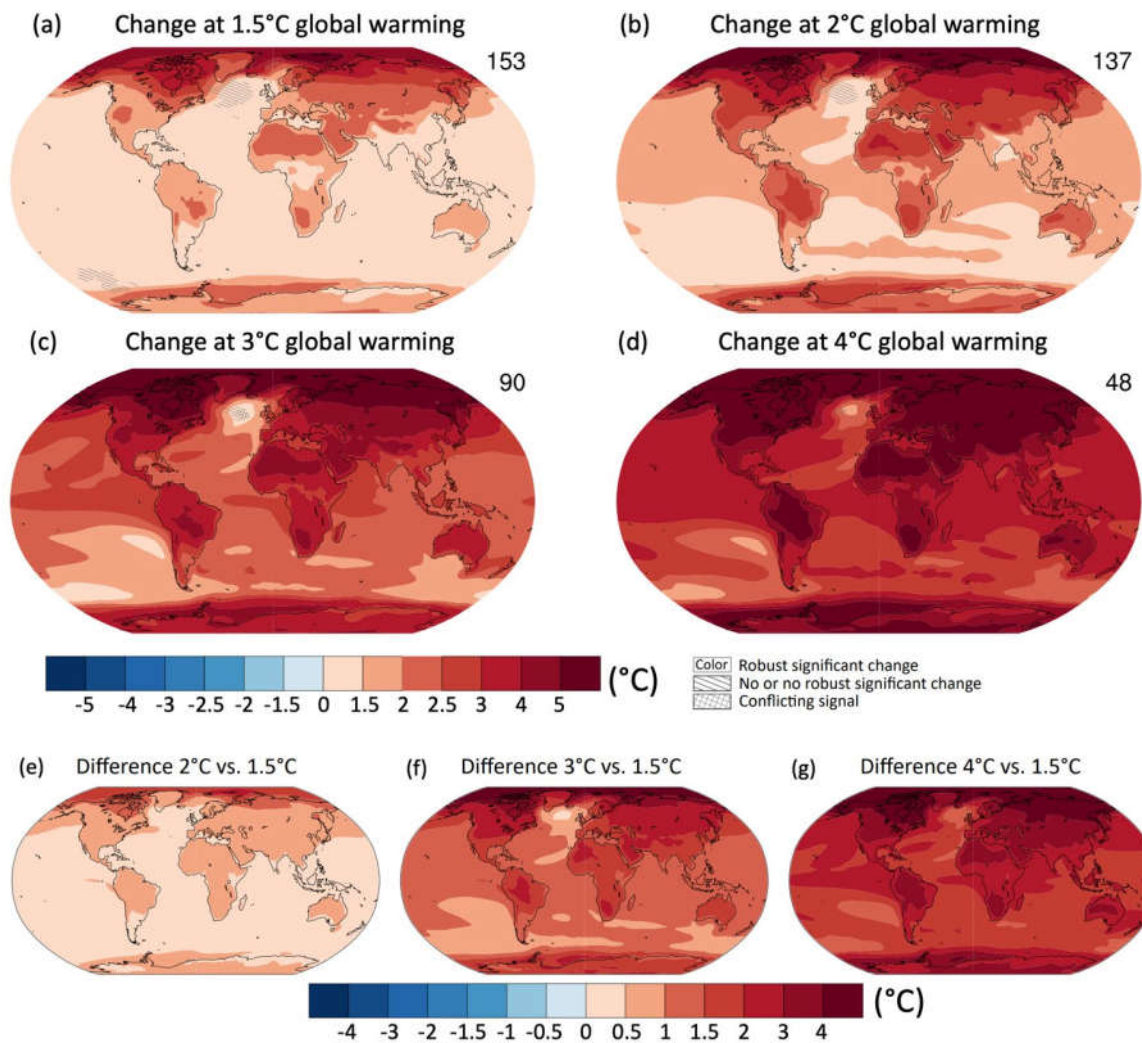


Projected spatial patterns of change in annual average near-surface temperature (°C) at different levels of global warming.

Figure 4.31: Projected spatial patterns of change in annual average near-surface temperature (°C) at different levels of global warming. Displayed are (a–d) spatial patterns of change in annual average near-surface temperature at 1.5°C, 2°C, 3°C, and 4°C of global warming relative to the period 1850–1900 and (e–g) spatial patterns of differences in temperature change at 2°C, 3°C, and 4°C of global warming compared to 1.5°C of global warming. The number of models used is indicated in the top right of the maps. No overlay indicates regions where the change is robust and *likely* emerges from internal variability, that is, where at least 66% of the models show a change greater than the internal-variability threshold (see Section 4.2.6) and at least 80% of the models agree on the sign of change. Diagonal lines indicate regions with no change or no robust significant change, where fewer than 66% of the models show change greater than the internal-variability threshold. Crossed lines indicate areas of conflicting signals where at least 66% of the models show change greater than the internal-variability threshold but fewer than 80% of all models agree on the sign of change. Values were assessed from a 20-year period at a given warming level, based on model simulations under the Tier-1 SSPs of CMIP6. Further details on data sources and processing are available in the chapter data table (Table 4.SM.1).

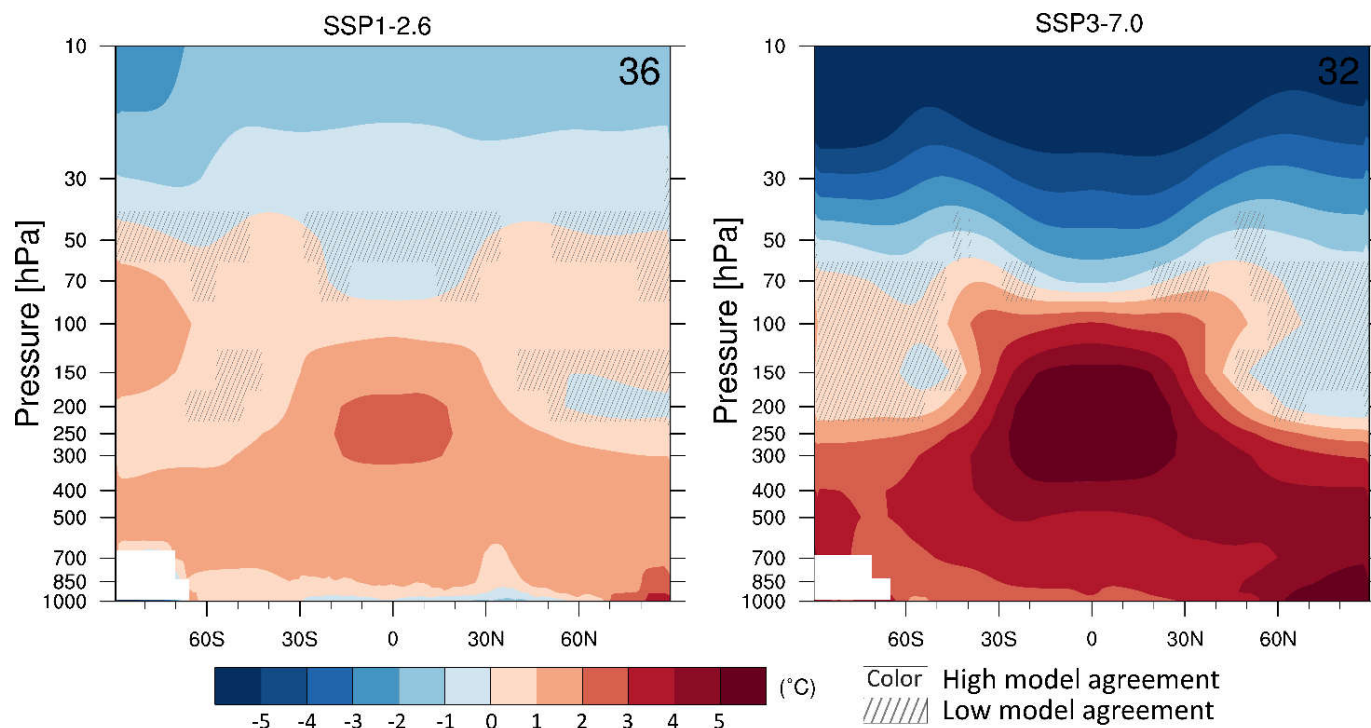


IPCC 2021, Chap. 4



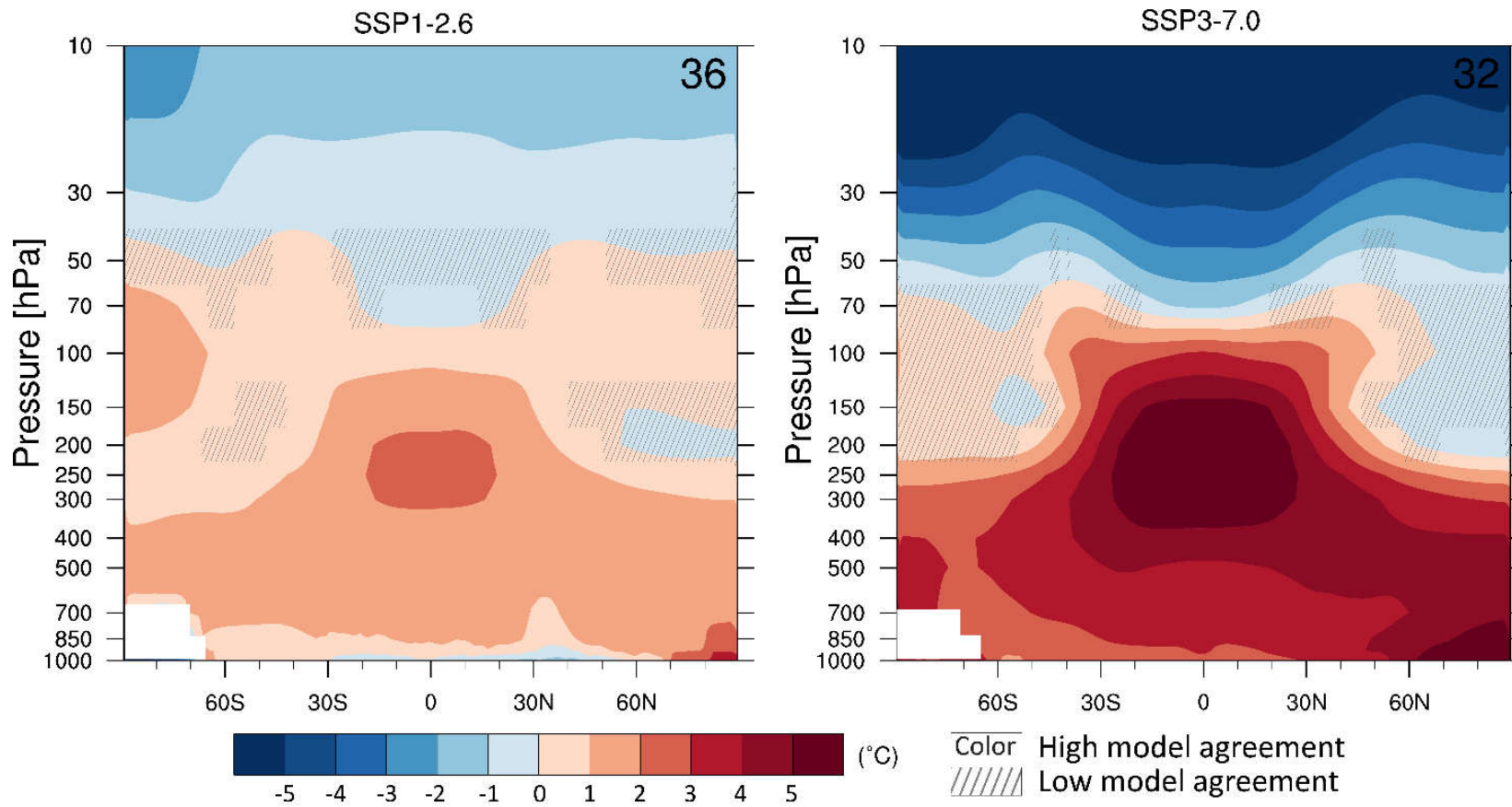
Long-term change of annual and zonal mean atmospheric temperature

Figure 4.22: Long-term change of annual and zonal mean atmospheric temperature. Displayed are multi-model mean change in annual and zonal mean atmospheric temperature ($^{\circ}\text{C}$) in 2081–2100 relative to 1995–2014 for (left) SSP1-2.6 and (right) SSP5-8.5. The number of models used is indicated in the top right of the maps. Diagonal lines indicate regions where less than 80% of the models agree on the sign of the change and no overlay where 80% or more of the models agree on the sign of the change. Further details on data sources and processing are available in the chapter data table (Table 4.SM.1).



IPCC 2021, Chap. 4





Chapter 4: Future global climate: scenario-based projections and near-term information

Continued

Nächste Vorlesung am 4. Mai 2022



Knowledge for Tomorrow